THE GEOLOGICAL SOCIETY OF AMERICA®

Discovery of Middle–Late Devonian and Early Permian magmatic events in East Asia and their implication for the Indosinian orogeny in South China: Insights from the sedimentary record

Xinchang Zhang[1,2], Yuejun Wang[2,†], Ron Harris[3], Yi Yan[1], and Yi Zheng[2]

[1]*Key Laboratory of Ocean and Marginal Sea Geology, Guangzhou Institute of Geochemistry, Chinese Academy of Sciences, Guangzhou 510640, China*

[2]*Guangdong Provincial Key Laboratory of Geodynamics and Geohazards, School of Earth Sciences and Engineering, Sun Yat-sen University, Guangzhou 510275, China*

[3]*Department of Geological Sciences, Brigham Young University, S389 Eyring Science Center, Provo, Utah 84602, USA*

ABSTRACT

Whether the driver of the Indosinian orogeny in the South China block was related to the evolution of the Paleotethyan Ocean or the Paleo-Pacific Ocean has been a point of much debate. We applied detrital zircon U-Pb dating to Permian–Triassic sedimentary rocks from South China to trace sediment provenance and to further test these models. Our results, combined with other published data from the Pingxiang, Youjiang, Yong'an, and Yongding Basins, show that 400–350 Ma and 300–260 Ma zircon grains are ubiquitous throughout the entirety of southern South China. This indicates regional magmatic events as potential sources. The discovery of Middle–Late Devonian and Early Permian igneous rocks, tuffs, and volcaniclastic rocks in Southeast Asia and Hainan Island implies the presence of two magmatic events (400–350 Ma and 300–260 Ma) within or beyond the southern margin of South China. This information, together with the mostly negative $\varepsilon_{Hf}(t)$ values of 400–350 Ma and 300–260 Ma zircon grains, arc-like geochemical signatures of the possible source rocks, and the regional geology of East Asia, suggests that they originated from sources related to Paleotethyan and even Proto-Tethyan subduction. Thus, Permian–Triassic sedimentation and the Indosinian orogeny in South China were largely controlled by the evolution of the Tethyan Ocean.

†Corresponding author: wangyuejun@mail.sysu.edu.cn.

INTRODUCTION

During the Late Permian to Triassic, several major continental blocks, including Sibumasu, Indochina, South China, and North China, ultimately were amalgamated (Fig. 1; Metcalfe, 1996, 2013; Lepvrier et al., 1997, 2004; Faure et al., 2014; Wang et al., 2018). This amalgamation controlled the tectonic framework of East Asia, as well as the construction of the basic tectonic pattern of the South China block by the end of the Indosinian orogeny (Ren, 1964, 1991; Zhang et al., 2013; Wang et al., 2013; Shu et al., 2015). However, during this time, the South China block was in the dynamic environment of eastern Tethys expansion and Pangea assembly, and surrounded by different plates, including the Paleotethyan Ocean to the west and the Paleo-Pacific Ocean to the southeast (Metcalfe, 2002, 2013; Li and Li, 2007; Wang et al., 2013, 2018; Faure et al., 2014). In part because of its complex tectonic position and later strong tectonic modification (e.g., during the Yanshanian movement, ca. 190–80 Ma; Chen and Jahn, 1998; Li and Li, 2007), the driver for the Indosinian orogeny in the South China block has long been a point of much debate.

Some authors have considered that orogenesis was driven by continental collisions, including the collision between the South China block and Indochina block (Fig. 2A; Lepvrier et al., 2004; Yang and He, 2012; Yang et al., 2012; Faure et al., 2014, 2016; Qiu et al., 2017), collision between the Sibumasu and Indochina blocks (Metcalfe, 2011, 2013), or intracontinental reworking with an indirect link to subduction of surrounding plates (Fig. 2B; Carter and Clift, 2008; Wang et al., 2005, 2013; Shu et al., 2008, 2009, 2015; Zhang et al., 2013). In contrast, others have argued that the deformation and magmatism in the South China block were influenced by the subduction of the Paleo-Pacific Ocean along the southeastern margin of the South China block (Fig. 2C; Carter and Clift, 2008; X.H. Li et al., 2006, 2012; Z.X. Li et al., 2012; Li and Li, 2007; Zhu et al., 2014; Pang et al., 2014; Jiang et al., 2015). However, the onset of Paleo-Pacific subduction is controversial (e.g., Taylor and Hayes, 1983; Engebretson et al., 1985; Li and Li, 2007; Hennig et al., 2017; Breitfeld et al., 2017). For example, Li and Li (2007) have speculated that this subduction started in the earliest Permian (ca. 280 Ma) or at least in the Triassic (Hennig et al., 2017; Breitfeld et al., 2017), whereas Engebretson et al. (1985) argued that it did not commence until the Early–Middle Jurassic (see also in Metcalfe, 1996, 2002; Veevers, 2004; Shu et al., 2015).

One way of resolving this problem is by investigating the sedimentary record in the South China block, to determine whether it is related to the convergence of the Paleotethys or influenced by the subduction of the Paleo-Pacific. Sedimentary sequences record significant information about their source rocks and can be further used to identify their depositional environment, tectonic setting, and continental growth (Spencer et al., 2016; X.C. Zhang et al., 2017; Breitfeld et al., 2018; Hennig et al., 2018). Thus, the Upper Permian to Upper Triassic sedimentary rocks that are now exposed in an area where the Paleotethys and Paleo-Pacific tectonic zones overlapped may provide one of the best opportunities for elucidating the geodynamic frame-

GSA Bulletin; https://doi.org/10.1130/B35032.1; 10 figures; 1 table; Data Repository item 2019018.

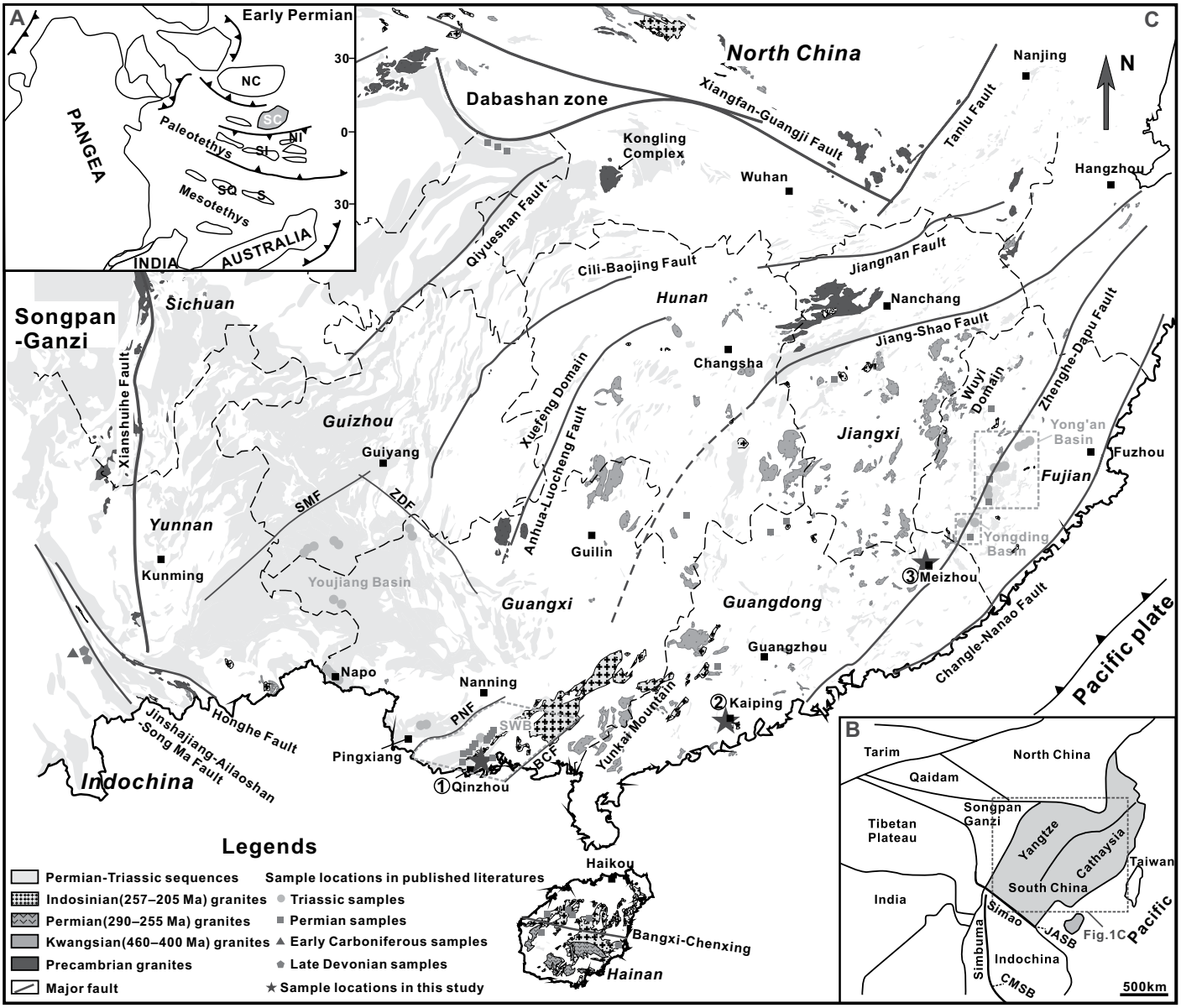

Figure 1. (A) Paleogeographic reconstruction of the Tethyan region for the Early Permian (modified from Metcalfe, 2013; Wang et al., 2018). Abbreviations: NC—North China block; SC—South China block; NI—Indochina block; SQ—South Qiangtang; SI—Simao; S—Sibumasu. (B) Tectonic framework of East Asia (modified from Metcalfe, 2002; Hu et al., 2015b). JASB—Jinshajiang–Ailaoshan–Song Ma belt; CMSB—Changning-Menglian and Chiangmai suture zone. (C) Simplified geological map of the South China block (modified from Yang et al., 2012; Wang et al., 2013; Hu et al., 2017). The locations of previous detrital zircon U-Pb age analyses are shown (Yang et al., 2012; Yang and He, 2012; Liang et al., 2013; X.H. Li et al., 2012; Hu et al., 2014, 2015a, 2015b; Wang et al., 2009; Wang et al., 2014). ZDF—Ziyun-Danchi fault; SMF—Shizong-Mile fault; BCF—Bobai-Cengxi fault; PNF—Pingxiang-Nanning fault; SWB—Shiwandashan Basin.

work of the South China block. In this study, we carried out detrital zircon U-Pb age dating and Hf isotope analysis of Upper Permian to Upper Triassic sedimentary rocks in the southeastern and southern South China block to determine their provenance (Fig. 1C). Together with a comprehensive analysis of the petrography and sedimentology of rocks exposed in the other basins in the South China block (e.g., Youjiang Basin, Shiwandashan Basin, Pingxiang Basin, and Laowangzhai region in the west side of Yunkai Mountain; Yong'an and Yongding Basins on the east side of Yunkai Mountain), we further discuss its tectonic setting and possibly two large-scale magmatic events that occurred in the Middle–Late Devonian and Early Permian, either within or outboard of the southern South China block.

GEOLOGICAL BACKGROUND

It is well acknowledged that the architecture of Asia resulted from the amalgamation of large continents, including the South China, North China, Sibumasu, and Indochina blocks, and several microcontinents (e.g., Metcalfe, 2013; Fig. 1A). These blocks are interpreted to have formed part of the north margin of Gondwana

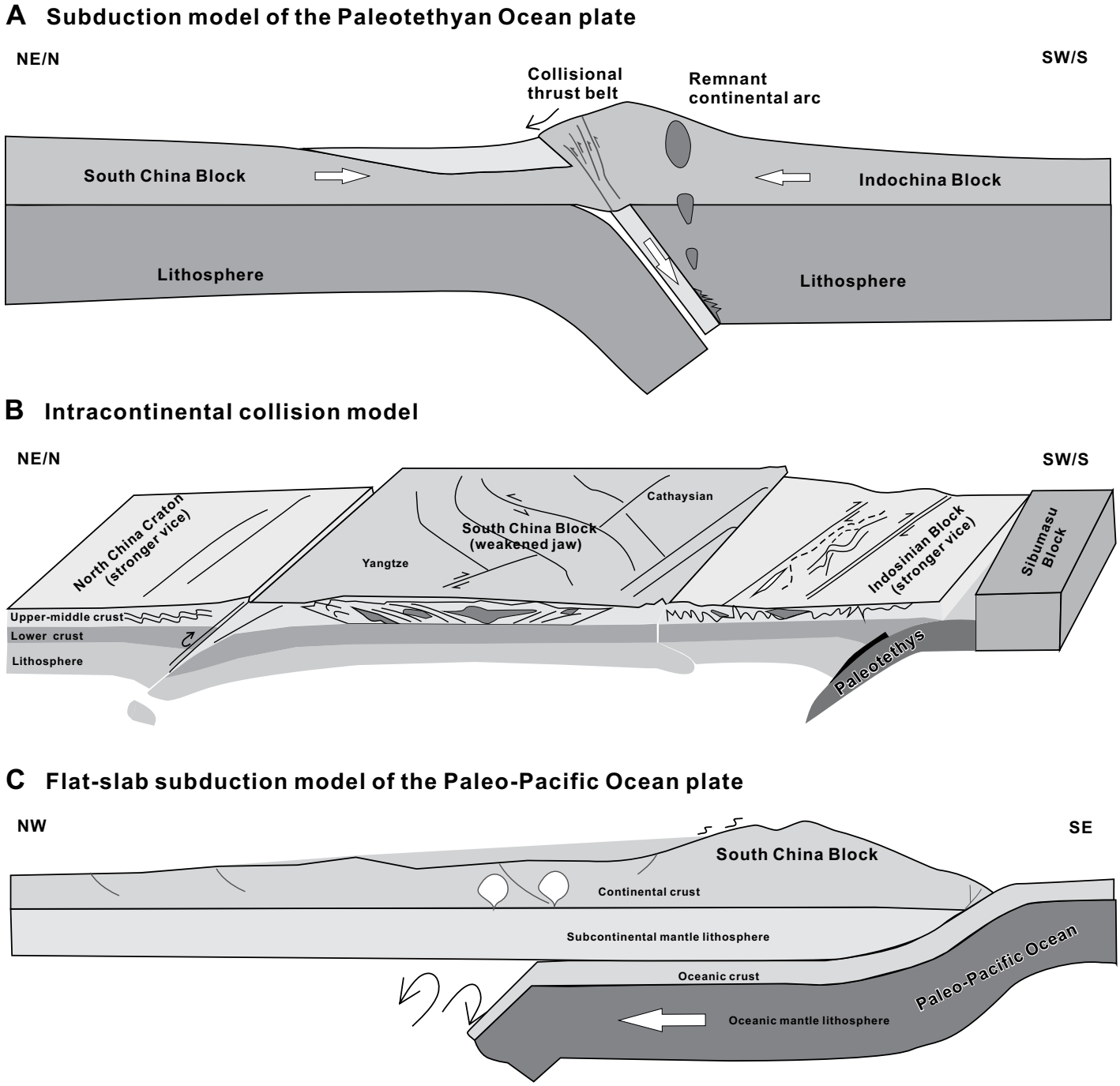

Figure 2. Summary of different tectonic models for an Indosinian event that has affected South China as proposed by (A) Yang et al. (2012) and Qiu et al. (2017), (B) Wang et al. (2013), and (C) Li and Li (2007).

in the early Paleozoic and to have rifted and separated from Gondwana during the opening of the Paleotethys in the Silurian–Devonian (Fig. 1; Cawood et al., 2013; Hara et al., 2010, 2012; Metcalfe, 2011, 2013; Spencer et al., 2016; Wang et al., 2018). They drifted northward across the ocean and finally accreted together to create the Pangea supercontinent, delineated by a series of Tethyan sutures (Hara et al., 2010, 2012; Metcalfe, 2011, 2013; Spencer et al., 2016; Wang et al., 2013, 2018). The Changning-Menglian-Inthanon suture zone represents a relict of the East Paleotethyan Ocean (Hara et al., 2012; Metcalfe, 2013; Wang et al., 2018). It separates the Simao-Indochina block to the east from the Sibumasu block to the west, and it extends from southwest Yunnan across northwest Laos into northwest Thailand (Fig. 1B). The Jinshajiang–Ailaoshan–Song Ma suture zone (JASB in Fig. 1B) is inferred to represent either a back-arc basin remnant or a branch of the East Paleotethyan Ocean, which was finally consumed in the Late Permian–Late Triassic (Jian et al., 2009a, 2009b; Lepvrier et al., 1997, 2004, 2008; Fan et al., 2010; Faure et al., 2014; Liu et al., 2015; Wang et al., 2018). This belt bounding the Indochina-Simao and South

China blocks likely extends southeastward to the Bangxi-Chenxing fault in Hainan Island (e.g., Faure et al., 2016). However, on the basis of investigations into the regional paleogeography of southwestern China, Carter et al. (2001) and Carter and Clift (2008) suggested that the Jinshajiang–Ailaoshan–Song Ma suture zone might represent only a reactivated zone during the collision of Sibumasu with Indochina. A Late Permian–Late Triassic amalgamation of the Indochina and South China blocks is favored here (Fig. 2A), because ophiolitic fragments, bedded cherts containing early Carboniferous radiolaria, volcano-sedimentary sequences, and subduction-related igneous rocks have been widely reported along this suture zone (e.g., Jian et al., 2009a, 2009b; Fan et al., 2010; Lepvrier et al., 2011; Metcalfe, 2002, 2013; Zi et al., 2012; Faure et al., 2014, 2016; Liu et al., 2015, 2017). In this subduction model of the Paleotethyan Ocean plate, the basins in the southern South China block are interpreted as a foreland basin receiving materials from the collisional belt between the South China block and Indochina blocks (Fig. 2A; Yang et al., 2012; Qiu et al., 2017). Furthermore, Wang et al. (2007b) have proposed that the driver of the Indosinian orogeny in the South China block was triggered by intracontinental convergence during the assembly of Pangea. In this case, the less competent South China orogen was squeezed between the more competent North China and Indochina blocks (Fig. 2B). Accordingly, this orogenic mechanism caused a large-scale positive flower structure involving top-to-the-SE and top-to-the-NW thrusting with a sinistral strike-slip component in the South China block (Chen, 1999; Yan et al., 2003; Wang et al., 2005, 2007b, 2013). Li and Li (2007) attempted to integrate the subduction and intracontinental collision hypotheses by invoking a flat-slab subduction model of the Paleo-Pacific Ocean plate to explain deformation and granite magmatism up to 1300 km from the inferred subduction zone (Fig. 2C). In this model, the SE-dipping thrusting, synorogenic magmatism, and foreland basin deposition propagated toward the cratonic interior in response to developing flat-slab subduction of the Paleo-Pacific Ocean plate (Fig. 2C).

Today, the South China block is bounded to the north by the Qinling-Dabie orogenic belt, a suture between the North China and South China blocks (Fig. 1; Metcalfe, 1996), and to the northwest by the Songpan-Ganzi fold system, which is interpreted to be a remnant oceanic basin from suturing of the North China and South China blocks (Meng and Zhang, 1999). The South China block is bordered by the Paleotethys tectonic zone to the southwest/south and by the Pacific Ocean plate to the southeast (Fig. 1). The South China block was formed by amalgamation of the Yangtze and Cathaysia blocks in the early Neoproterozoic (Fig. 1; Charvet et al., 1996; Zhao and Cawood, 1999; Li et al., 2009; Wang et al., 2013). The Jiangshan-Shaoxing fault (Jiang-Shao fault) is thought to be the boundary between the two blocks in the northeastern South China block, while its southwestern extension is unclear (Fig. 1C; Charvet et al., 1996, 2010; Li et al., 2009). The Yangtze and Cathaysia blocks have different crystalline basement compositions. The oldest rocks are the Kongling Complex near the Yangtze Gorge Dam in the Yangtze block, consisting of Mesoarchean to early Paleoproterozoic high-grade metamorphic tonalite-trondhjemite-granodiorite (TTG) gneisses, metasedimentary rocks, and amphibolites (Gao et al., 1999; Qiu et al., 2000; Zheng et al., 2006). Minor ca. 1.7 Ga volcanic rocks (Greentree and Li, 2008) and ca. 1.1–0.9 Ga magmatic rocks outcrop on the western and southeastern margins of the Yangtze block (Li et al., 2009). Neoproterozoic (0.84–0.74 Ga) granites, mafic rocks, and sedimentary rocks are widespread and are mostly distributed around the margins of the Yangtze block (e.g., Li et al., 2010). In the Cathaysia block, the oldest crystalline basement rocks are the ca. 1.8 Ga gneisses and amphibolites of the Badu Group, which are limited to the southern Zhejiang–northwestern Fujian area (Fig. 1C; Yu et al., 2009, 2010, 2012). Mesoproterozoic (ca. 1430 Ma) rocks, consisting mainly of granodiorites, are restricted to Hainan Island (Li et al., 2002, 2008). The Kwangsian granitic rocks (mostly dated at 450–420 Ma) are the primary product of Paleozoic magmatism and are predominantly exposed to the east of the Xuefeng Domain (Fig. 1C; Chen and Jahn, 1998; Charvet et al., 1996, 2010; Wan et al., 2010; Wang et al., 2007a, 2007b, 2013). The Indosinian granitic plutons widely outcrop in the region between the Xuefeng Domain and Yunkai Domain (Fig. 1C). These granites intruded the pre-Triassic strata as stocks and batholiths and are mainly dated at ca. 250–200 Ma (Wang et al., 2007a, 2013).

MAJOR BASINS IN THE SOUTHERN SOUTH CHINA BLOCK

In the South China block, series of basins have been identified, such as Youjiang (also named Nanpanjiang basin) and Shiwandashan Basins, and other small basins, i.e., Pingxiang, Yongding, and Yong'an Basins (Fig. 1C). These basins are separated by major faults and/or differential uplift and can be subdivided into two greater basins separated by the NE/ENE-trending Yunkai Mountain (Qiu et al., 2017; Hu et al., 2017). Yunkai Mountain is located in western Guangdong and eastern Guangxi Provinces (Fig. 1C) and is commonly believed to be a component of the Cathaysia block (Chen and Jahn, 1998). The Precambrian metamorphic basement of Yunkai Mountain, which contains abundant Neoarchean zircon grains (Yu et al., 2010), is covered unconformably by Devonian and younger strata, all intruded by early Paleozoic and Permian–Triassic granites, and affected by associated tectonothermal events (BGMRGD, 1988; Wan et al., 2010).

To the west of Yunkai Mountain, Youjiang Basin lies close to the southwestern margin of the South China block and is bounded by the Ziyun-Danchi fault to the northeast and the Shizong-Mile fault to the northwest (Fig. 1C; Yang et al., 2012; Hu et al., 2017). Permian to Early Triassic sedimentation within the basin was dominated by marine clastic and volcanic clastic strata and isolated carbonate platforms (Yang et al., 2012). Middle Triassic sedimentation consists of a thick siliciclastic succession dominated by medium- to fine-grained terrigenous turbidites and shales (BGMRGX, 1985; Duan et al., 2018). By the end of the Late Triassic, marine sedimentation had ended. Sedimentation was then dominated by fluvial systems and a shallow-marine shelf clastic environment (Carter and Clift, 2008). In addition, the northeast-trending Shiwandashan Basin (Fig. 1C) is mainly composed of a late Paleozoic–Middle Triassic sedimentary succession of sandstone and shale. It is separated from Yunkai Mountain to the southeast by the Bobai-Cenxi fault and from the Youjiang Basin in the northwest by the Pingxiang-Nanning fault (Fig. 1C; Hu et al., 2015a). In the Qinzhou section of this basin, the Late Permian–Early Triassic succession is an unconformably bound package overlain by the Upper Triassic strata and underlain by Devonian siliciclastic rocks (Fig. 3; BGMRGX, 1985). The Upper Permian strata include four formations (in ascending order), P_2^a, P_2^b, P_2^c, and P_2^d, which show features of terrigenous paralic deposition of shore facies (Fig. 3; Liang and Li, 2005).

To the east of Yunkai Mountain, Early Permian strata in the Kaiping area are dominated by shallow-marine carbonates (Fig. 3). A marked change in sedimentation occurred in the Late Permian with deposition of muddy shale with interbedded medium- to thick-bedded, fine-medium sandstone (Longtan Formation; BGMRGD, 1988). The overlying Early Triassic Formation consists mainly of yellow to pink muddy shale intercalated with siltstone. The succession is overlain unconformably by Lower Jurassic conglomerates and quartz sandstones, siltstone, and muddy shale (Fig. 3; BGMRGD, 1988). In the Meizhou area (Fig. 1C), the Lower Permian Qixia Formation consists of shallow-marine carbonates pass-

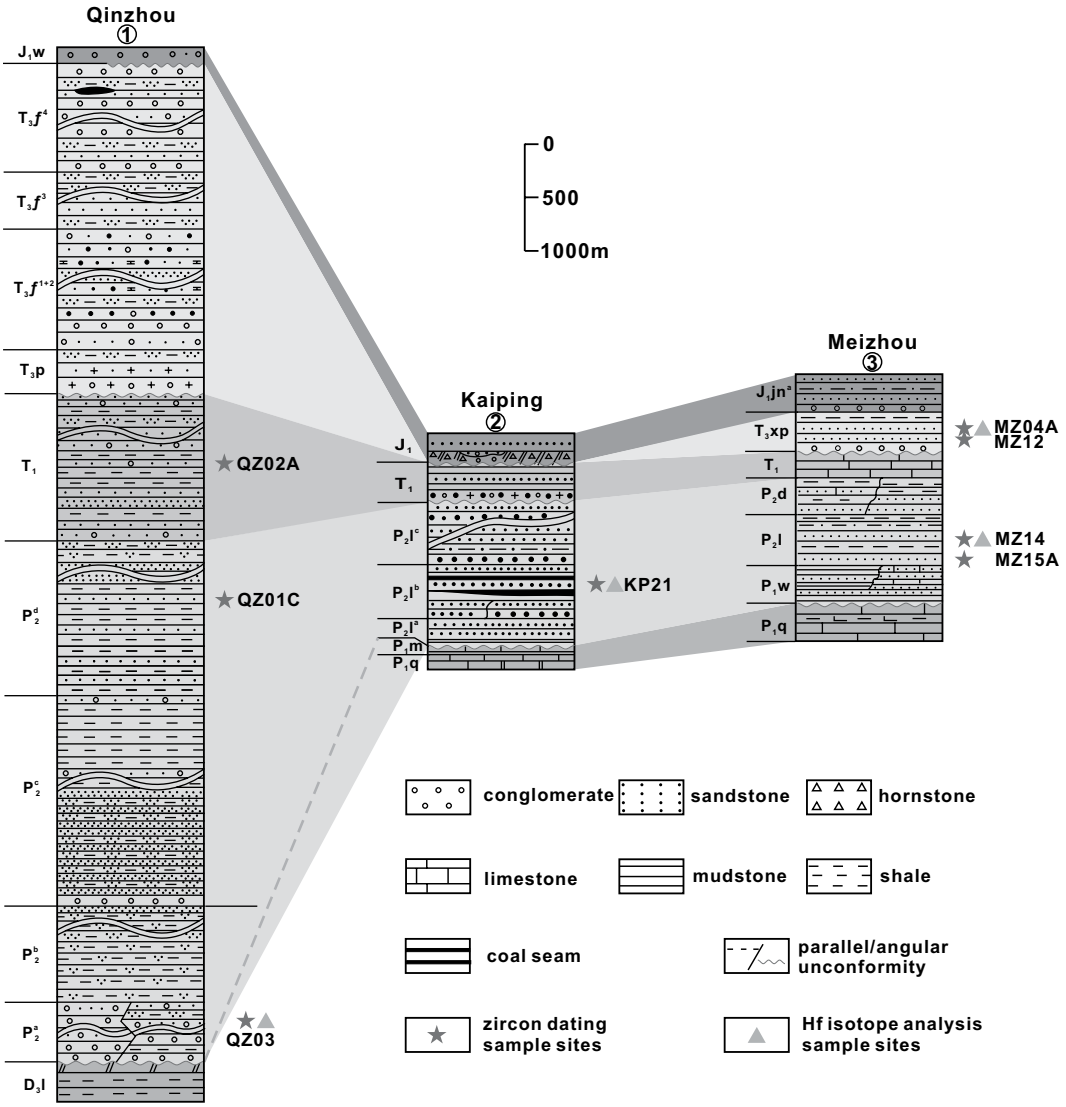

Figure 3. Regional stratigraphic columns of Permian to Triassic successions in the South China block with positions of sandstone samples. Positions of the columns are shown in Figure 1. Stratigraphic units: D_3l—Liujiang Formation; P_1q—Qixia Formation; P_1m—Maokou Formation; P_1w—Wenbishan Formation; P_2^a, P_2^b, P_2^c, P_2^d—four formations of Late Permian in ascending order; P_2l—Longtan Formation; P_2d—Dalong Formation; T_1—Early Triassic Formation; T_3p—Pingtong Formation; T_3f—Feixianguan Formation; T_3xp—Xiaoping Formation; J_1—Early Jurassic Formation; J_1w—Wangmen Formation; J_1jn—Jinji Formation.

ing up into shallow-water siliciclastic units of the Wenbishan Formation. The Middle Permian Formation is composed of gray bedded mudstones and siltstone (Fig. 3). The geology east of Yunkai Mountain is complex because of later tectonic movements (e.g., Yanshanian movement), but on the whole, sedimentation in the basins is mainly composed of Early Permian carbonate and Late Permian to Late Triassic clastic sediments with delta, littoral, or coastal swamp facies (BGMRGD, 1988).

SAMPLING AND ANALYTICAL METHOD

Three sections through the Upper Permian to Upper Triassic successions in the Kaiping, Meizhou, and Qinzhou areas were measured and sampled for detrital provenance analysis (Figs. 1 and 3). Weathered surfaces were removed from samples prior to analysis. The Gazzi-Dickinson method was used to point count eight sandstones, with ~300 grains counted from each sample (Dickinson and Suczek, 1979). Grains and clasts <60 μm were not counted, and the resulting data are available in Supplemental Table S1.[1]

Zircon U-Pb dating and in situ Hf isotopic analysis were performed at the Key Laboratory of Isotope Geochronology and Geochemistry, Guangzhou Institute of Geochemistry, Chinese Academy of Sciences. The laser ablation–inductively coupled plasma–mass spectrometry (LA-ICP-MS) system was composed of an Agilent 7500a ICP-MS coupled with a Resonetics RESOLution 50-M ArF excimer laser source (λ = 193 nm). It can wash out 99% of the signal in less than 1.5 s due to its innovative sample cell design (Xia et al., 2013). The multicollector (MC) ICP-MS was fitted with a collector block containing eight variable-position Faraday cups, one fixed central Faraday cup, and eight ion counters. This collector system has a relative mass range of more than 17%, allowing simultaneous acquisition of ion signals ranging from mass ^{202}Hg to ^{238}U, an important factor in obtaining highly precise and accurate U-Pb age determinations. A newly designed interface cone assemblage, consisting of a Jet sample cone and X skimmer cone (from Thermo Scientific), and a large dry interface pump (100 m^3/h pumping speed) were equipped with the machine to further improve the instrument sensitivity (Zhang et al., 2014). Helium was used as the carrier gas to enhance the transport efficiency of the ablated material. The helium carrier gas inside the ablation cell was mixed with argon gas before entering the ICP-MS to maintain stable and optimum excitation conditions. Analyses were conducted

[1]GSA Data Repository item 2019018, Supplemental Tables S1–S3, is available at http://www.geosociety.org/datarepository/2019 or by request to editing@geosociety.org.

with a beam diameter of 24 μm; each analysis included ~30 s blank gas measurement followed by a further 30 s analysis time when the laser was switched on. The common Pb composition could not be accurately corrected for due to its very low counts (^{204}Pb) and interference from ^{204}Hg in gas. Harvard zircon 91500 (Wiedenbeck et al., 1995) was used to calibrate the U-Th-Pb ratios and absolute U abundances. The zircon standard Plešovice (Sláma et al., 2008) was used to monitor unknown samples (mean ^{206}Pb/^{238}U age = 337.6 ± 1.3 Ma, mean square of weighted deviations [MSWD] = 0.078, n = 109). They always gave ages within 3% error of their recommended values. Isotope ratios were calculated using ICPMSDataCal 7.7 (Liu et al., 2010). The relative probability age of detrital zircon grains was processed using Isoplot (version 3.23; Ludwig, 2003). Errors for individual analyses are given as 1σ. Systematic uncertainty for propagation was 2%. Concordance was calculated as 100 – 100 × abs(^{207}Pb/^{235}U age – ^{206}Pb/^{238}U age)/(^{206}Pb/^{238}U age). Thus, we only discuss the data in which the ^{207}Pb/^{235}U age and ^{206}Pb/^{238}U age were concordant within uncertainty. Ages were calculated using ^{207}Pb/^{206}Pb and ^{206}Pb/^{238}U data for the older (>1 Ga) and younger (<1 Ga) zircon grains, respectively (Griffin et al., 2004). Lu-Hf isotopic analyses were obtained on the same zircon grains that were previously analyzed for U-Pb isotopes. Ratios used to correct measured data were 0.79381 for ^{176}Yb/^{173}Yb and 0.02656 for ^{176}Lu/^{175}Lu (Segal et al., 2003; Wu et al., 2006). The standard zircon Penglai was also analyzed as an unknown to check the reliability of the method (mean ^{176}Hf/^{177}Hf = 0.282895 ± 0.000007, MSWD = 3.8, n = 48). The initial ^{176}Hf/^{177}Hf ratios were calculated using the decay constant for ^{176}Lu of 1.867 × 10^{-11} yr^{-1} (Scherer et al., 2001). The zircon U-Pb ages and the present-day chondritic values of ^{176}Hf/^{177}Hf = 0.282772 and ^{176}Lu/^{177}Hf = 0.0332 (Blichert-Toft et al., 1997) were used for calculating $\varepsilon_{Hf}(t)$. Single-stage model ages (T_{DM1}) were calculated relative to depleted mantle with a present-day $(^{176}Lu/^{177}Hf)_{DM}$ = 0.0384 and $(^{176}Hf/^{177}Hf)_{DM}$ = 0.28325 (Vervoort and Blichert-Toft, 1999; Griffin et al., 2000). Two-stage model ages (T_{DM}^{C}) were calculated for the source rock of magma by assuming a mean ^{176}Lu/^{177}Hf value of 0.015 for the average continental crust (Griffin et al., 2002).

ANALYTICAL RESULTS

Petrographic Analysis

The mineral compositions of all samples are reported in Supplemental Table S1 (see footnote 1). Sample KP21 was collected from the Kaiping area. It is a reddish fine-grained sandstone sample of Late Permian age, consisting of ~60% quartz, ~5% feldspar, and ~35% lithic fragments. The feldspar records metasomatism to muscovite. The shape of the grains is angular to subrounded with lots of clasts tending to be poorly sorted with a muddy matrix. Samples MZ14 and MZ15A (Late Permian age) and samples MZ04A and MZ12 (Late Triassic age) were collected from the Meizhou area in northeastern Guangdong Province. These sandstone samples are similar and show high maturity, with more than 90% quartz, ~1% muscovite, and rare feldspar and lithic fragments (sedimentary, metamorphic, and volcanic fragments). The shape of the detrital grains is rounded to subrounded and the quartz particles are in contact with each other, which means that these grains are recycled and have been transported over long distances. Samples QZ01C, QZ03, and QZ02A were collected from the Qinzhou area of the Shiwandashan Basin. These sandstones are poorly sorted with subangular to angular detrital grains. Sample QZ01C is a cinerous fine-grained graywacke of Late Permian age. The major components are monocrystalline quartz (~62%) and lithic fragments (~34%), with minor polycrystalline quartz and feldspar. Sample QZ03, from the lower section of Upper Permian strata, is dominated by monocrystalline quartz (~68%) with lithic fragments (~25%) and trace amounts of polycrystalline quartz (~1%) and feldspar (~5%). Sample QZ02A is a fine-grained sandstone sample of Early Triassic age and is composed of monocrystalline quartz (~58%) with minor polycrystalline quartz (~3%), lithic fragments (~36%), and feldspar (~2%; Supplemental Table S1 [footnote 1]; Fig. 4).

Zircon U-Pb Ages and Lu-Hf Isotopes

Zircon grains extracted from the samples are light yellow to colorless. These grains are usually 80 μm to 200 μm long, with aspect ratios of 1:1–3:1. The shapes of studied zircon grains range from subrounded to angular. The internal structure of most of the grains shows oscillatory zoning (Fig. 5), suggesting a magmatic origin. Some metamorphic zircon grains were recognized from homogeneous internal structure. The majority of the zircon grains have Th/U >0.1, which also is indicative of an igneous origin, and some grains show Th/U <0.1, corresponding to metamorphic origins (Fig. 6; Rubatto, 2002). Some of the metamorphic grains have some enclaves, rounded growth lines, and round-shaped kernel. Detailed age and Lu-Hf isotope data for these samples are listed in Supplemental Tables S2 and S3 (see footnote 1).

Sample KP21 from Kaiping (P_2) (GPS: 22°17′18.8″N, 112°35′29.7″E)

In total, 50 detrital zircon grains were analyzed for this sample, which yielded 49 concordant ages (3071–261 Ma) with two major peaks at ca. 279 Ma and ca. 395 Ma. Subordinate age peaks are present at ca. 897 Ma, ca. 1126 Ma, and ca. 958 Ma, with some scattered ages between 1100 Ma and 2500 Ma (Fig. 7A).

Forty-nine Hf isotope analyses of 49 zircon grains were made for sample KP21. Zircon grains with the ca. 279 Ma age peak (300–260 Ma) exhibit $\varepsilon_{Hf}(t)$ values of –7.66 to +3.36, yielding T_{DM}^{C} model ages ranging from 1.07 to 1.79 Ga. The 400–350 Ma zircon grains have negative $\varepsilon_{Hf}(t)$ values from –10.28 to –1.39, with T_{DM}^{C} model ages from 1.48 to 2.04 Ga. The Precambrian zircon grains have $\varepsilon_{Hf}(t)$ values of –10.18 to +9.77, and a corresponding large range of T_{DM}^{C} model ages from 1.30 to 3.19 Ga (Fig. 8).

Samples QZ01C and QZ03 from Qinzhou, Shiwandashan Basin (P_2) (GPS: 21°45′14.3″N, 108°13′35.4″E; GPS: 21°44′31.7″N, 108°3′4.1″E)

In total, 55 detrital zircon grains from sample QZ03 were analyzed and yielded 54 concordant ages. These concordant ages have a range from early Paleozoic to Neoarchean (ca. 2831–414 Ma) with two major peaks at ca. 439 Ma and 991 Ma, two minor peaks at ca. 620 Ma and ca. 1114 Ma, scattered ages between 1763 Ma and 2460 Ma, and one Neoarchean zircon grain at 2831 Ma (Fig. 7B).

The 60 detrital zircon grains from sample QZ01C yielded 59 concordant ages (ca. 3221–424 Ma) with two significant age peaks at ca. 435 Ma and 971 Ma. Minor age peaks are shown at ca. 530 Ma, ca. 625 Ma, and ca. 810 Ma (Fig. 7C).

Fifty Hf isotope analyses of 50 zircon grains were made for sample QZ03. The grains within the 439 Ma age peak (474–414 Ma) have $\varepsilon_{Hf}(t)$ values ranging from –10.71 to –1.54 and T_{DM}^{C} model ages from 1.51 to 2.39 Ga. The 1100–962 Ma age group has $\varepsilon_{Hf}(t)$ values ranging from –13.02 to +9.01 and T_{DM}^{C} model ages from 1.28 to 2.66 Ga. The 2500–2400 Ma zircon grains have $\varepsilon_{Hf}(t)$ values of –4.68 to +1.04 with T_{DM}^{C} model ages from 2.86 to 3.23 Ga (Fig. 8).

Sample QZ02A from Qinzhou, Shiwandashan Basin (T_1) (GPS: 21°43′58.6″N, 108°07′41.7″E)

In total, 55 detrital zircon grains from this sample were analyzed, and 52 concordant ages were found, varying from 423 to 3376 Ma. Two main age peaks of 432 Ma and 968 Ma together with two subordinate peaks of 514 Ma and 793 Ma were recognized, as well as some

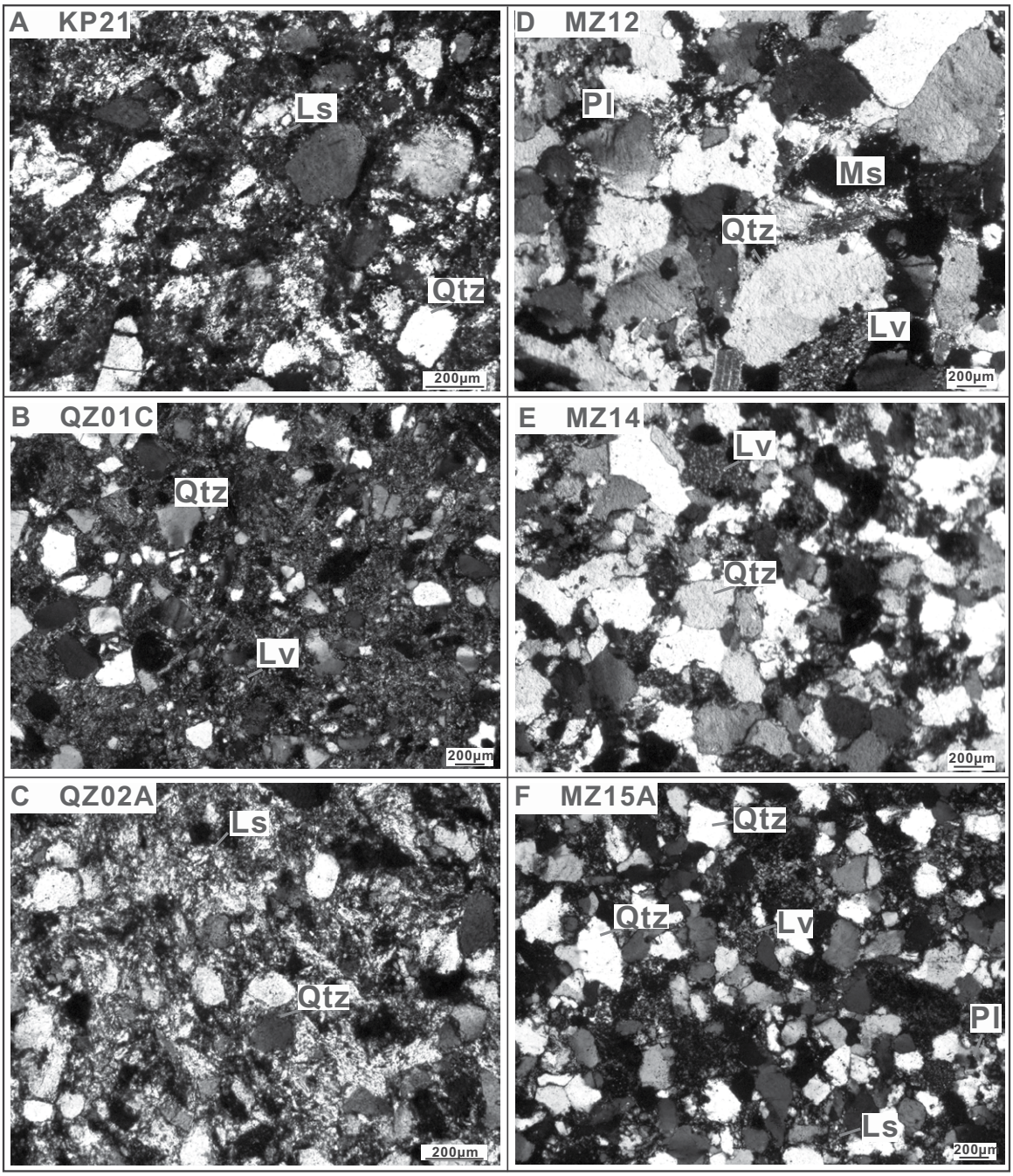

Figure 4. Thin section petrography of some samples. All images are under cross-polarized light. Abbreviations for minerals: Qtz—quartz; Pl—plagioclase; Ms—muscovite; Ls—sedimentary fragments; Lv—volcanic fragments; Lm—metamorphic fragments.

scattered ages between 1600 Ma and 2800 Ma (Fig. 7D).

Forty-eight Hf isotope analyses of 48 zircon grains were conducted. The 480–400 Ma zircon grains have $\varepsilon_{Hf}(t)$ values from –10.46 to +1.22 and T_{DM}^{C} model ages from 1.34 to 2.08 Ga, while the Precambrian zircon grains have $\varepsilon_{Hf}(t)$ values ranging from –23.64 to +8.99 and T_{DM}^{C} model ages from 1.37 to 3.32 Ga (Fig. 8).

Samples MZ14 and MZ15A from Meizhou (P_2) (GPS: 24°29′23.7″N, 116°10′54.3″E; GPS: 24°29′32.2″N; 116°10′10.4″E)

In total, 55 detrital zircon grains analyzed for sample MZ14 yielded 52 concordant ages (ca. 3539–259 Ma) with an age peak at ca. 294 Ma and a shoulder age peak at ca. 373 Ma. Two minor age peaks are shown at ca. 440 Ma and ca. 943 Ma (Fig. 7E).

Also, 55 detrital zircon grains were analyzed for sample MZ15A, which yielded 53 concordant ages (ca. 2524–260 Ma) and three age populations with age peaks at ca. 261 Ma, ca. 376 Ma, and ca. 1867 Ma, along with three subordinate age peaks at ca. 422 Ma, ca. 919 Ma, and ca. 2494 Ma (Fig. 7F).

Thirty-eight zircon grains (MZ14) with concordant ages were analyzed for Hf isotopes.

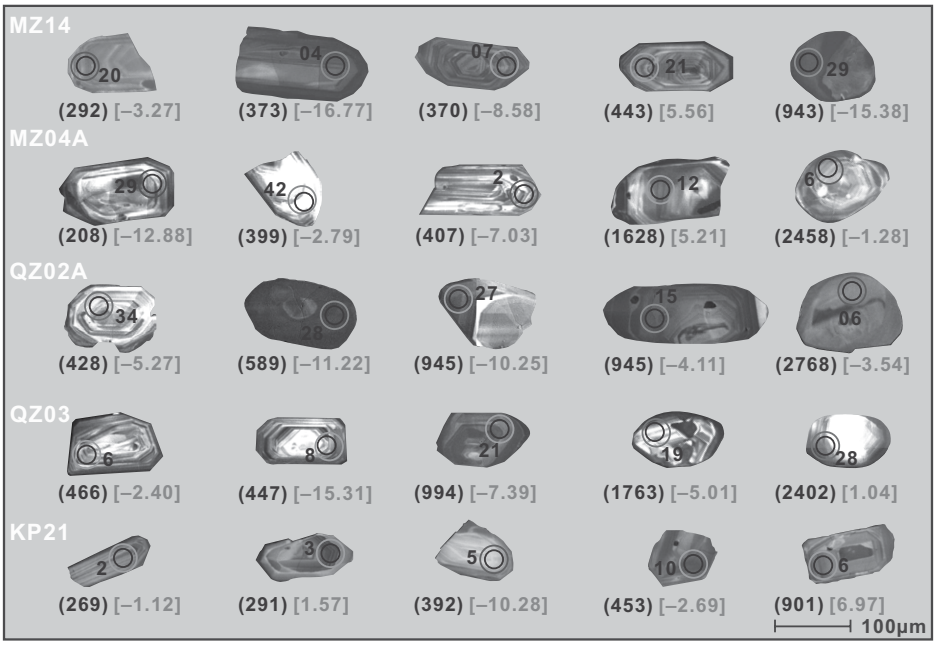

Figure 5. Representative cathodoluminescence (CL) images showing internal structure and morphology of the detrital zircon grains used for U-Pb age dating and in situ Lu-Hf isotope analysis. Small and large circles indicate the laser ablation–multicollector–inductively coupled plasma–mass spectrometry (LA-MC-ICP-MS) analytical spots for U-Pb and Lu-Hf isotope analysis, respectively. Numbers near the CL images are the ordinal number of analysis point. Numbers below the analytical spots are the U-Pb ages (within parentheses), and $\varepsilon_{Hf}(t)$ values (within large brackets).

The 294–276 Ma zircon grains have $\varepsilon_{Hf}(t)$ values from –13.74 to +4.63 and T_{DM}^{C} model ages from 1.05 to 2.18 Ga, indicating that their parent magmas were mainly produced by reworking of 2.18–1.05 Ga continental crust. The 381–366 Ma zircon grains have only negative $\varepsilon_{Hf}(t)$ values from –19.06 to –8.58 with T_{DM}^{C} model ages from 1.91 to 2.58 Ga. The 2500–1800 Ma zircon grains have $\varepsilon_{Hf}(t)$ values of –13.8 to +9.19, and a corresponding large range of T_{DM}^{C} model ages from 1.95 to 3.84 Ga (Fig. 8).

Samples MZ12 and MZ04A from Meizhou (T_3) (GPS: 24°34′19.5″N, 116°21′2.1″E; GPS: 24°32′32.9″N, 116°3′55″E)

In total, 50 detrital zircon grains from sample MZ12 were analyzed, and 49 concordant ages were found, varying from ca. 291 to 2666 Ma. The ages mainly cluster in the range of 478–435 Ma, with a major peak at 445 Ma and a number of subordinate peaks at ca. 299 Ma, ca. 376 Ma, ca. 949 Ma, and ca. 1874 Ma (Fig. 7G).

Also, 55 analyses of 55 zircon grains were obtained for sample MZ04A, and 50 grains gave concordant analyses within uncertainties. The analyzed ages were between 205 Ma and 2639 Ma. Eighteen of the analyzed zircon grains were dated at 410–399 Ma, forming a significant age peak at ca. 402 Ma. Subordinate age peaks were present at ca. 205 Ma and ca. 692 Ma (Fig. 7H).

Forty-four dated zircon grains from sample MZ04A were analyzed for Hf isotopes. The zircon population within the significant 404 Ma age peak exhibited only negative $\varepsilon_{Hf}(t)$ values of –13.60 to –7.03, yielding T_{DM}^{C} model ages ranging from 1.84 to 2.25 Ga. The subordinate age peak of ca. 399 Ma zircon grains showed $\varepsilon_{Hf}(t)$ values of –16.77 to –2.79, and a corresponding large range of T_{DM}^{C} model ages from 1.57 to 2.45 Ga (Fig. 8).

DISCUSSION

Provenance of Pre–Middle Devonian Detrital Zircon Grains

The 417 zircon grains from eight sandstone samples in the South China block yielded a wide range of U-Pb ages from Archean (ca. 3500 Ma)

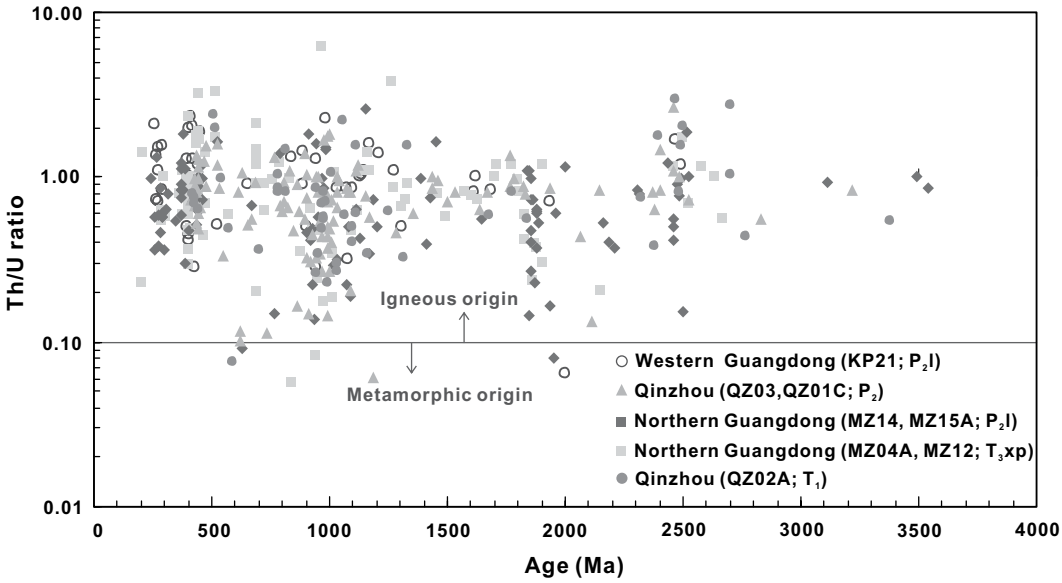

Figure 6. Zircon age and Th/U relationship diagram for the Late Permian–Late Triassic samples in southern and southeastern South China. See Figure 3 caption for unit abbreviations.

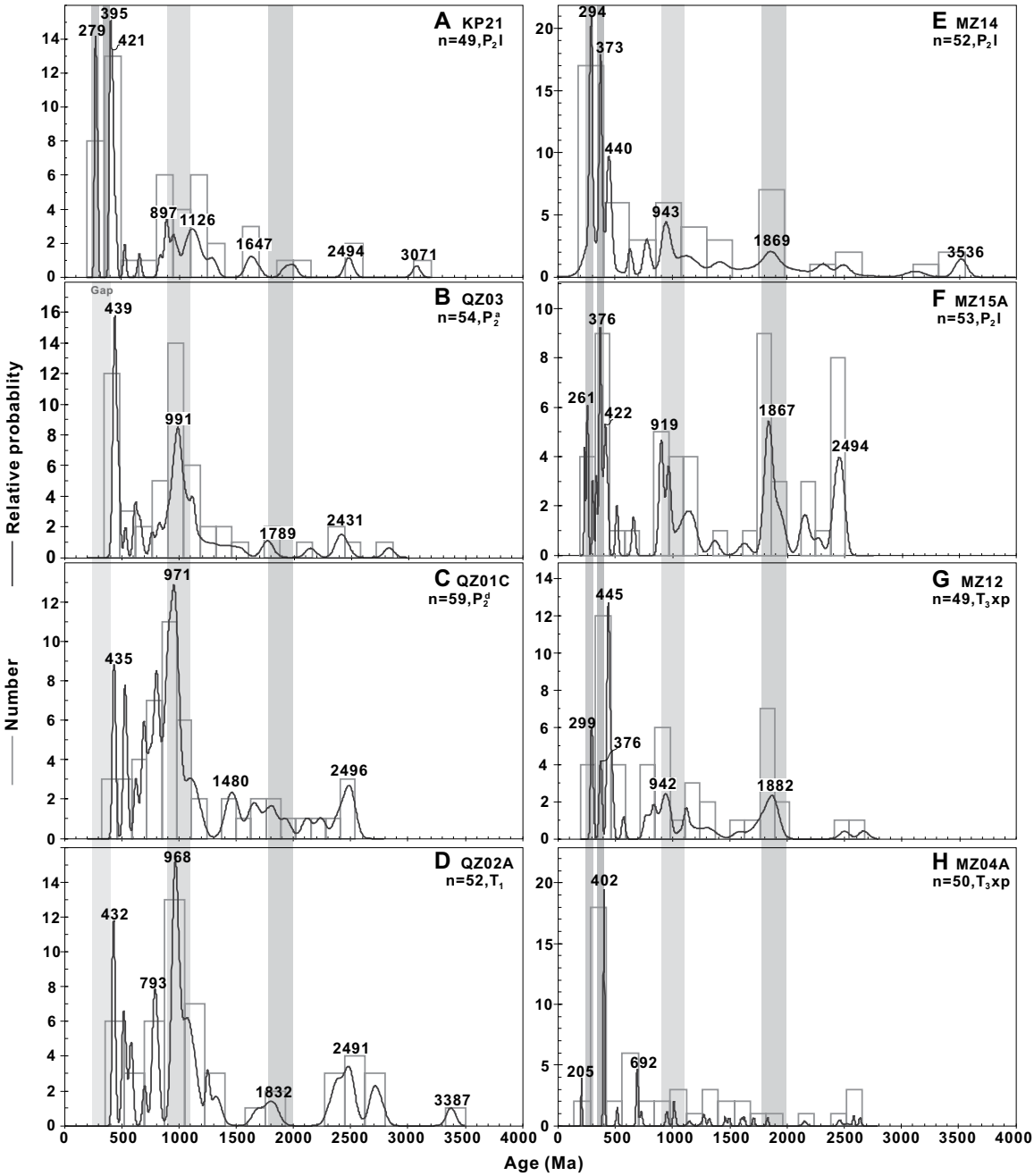

Figure 7. U-Pb relative probability diagrams of detrital zircon analytical results. Plots show concordant ages, with $^{206}Pb/^{238}U$ used for ages younger than 1000 Ma and $^{207}Pb/^{206}U$ age for older grains. Errors are quoted at the 1σ level. See Figure 3 caption for unit abbreviations.

to Mesozoic (ca. 205 Ma). The pre–Middle Devonian zircon grains (>400 Ma) are dominated by two major Neoproterozoic and late Paleozoic age peaks at 460–400 Ma and 1100–890 Ma, along with a subordinate late Paleoproterozoic peak at 1870–1830 Ma (Fig. 7).

The 54 zircon grains in this study are of Archean and Paleoproterozoic age (ca. 3.5–2.0 Ga). Considering Archean rocks in the South China block are scarce and are only found in the Kongling Complex within the Yangtze block (Gao et al., 1999; Qiu et al., 2000; Zheng et al., 2006), and the Yangtze block was widely covered by carbonate deposits in the Late Permian–Early Triassic (Li and Li, 2007; X.H. Li et al., 2012), we propose that zircon grains with these ages were most likely recycled from the older strata in the Cathaysia block. The late Paleoproterozoic zircon grains, with ages ranging from 2.0 to 1.7 Ga, are rare in the sandstones in the Kaiping and Qinzhou areas (~8.3% and ~4.8%, respectively), but they constitute a significant age group in the sandstones in the Meizhou area (~8%–20.8%, average 12.7%), as well as in the Yong'an and Yongding Basins in Fujian Province (Figs. 7 and 9; X.H. Li et al., 2012; Hu et al., 2015b; this study). This age feature is consistent with the limited Paleoproterozoic granitoids in the Wuyi Domain (Fig. 1C; Wan et al., 2007; Yu et al., 2009, 2012). Furthermore, zircon grains

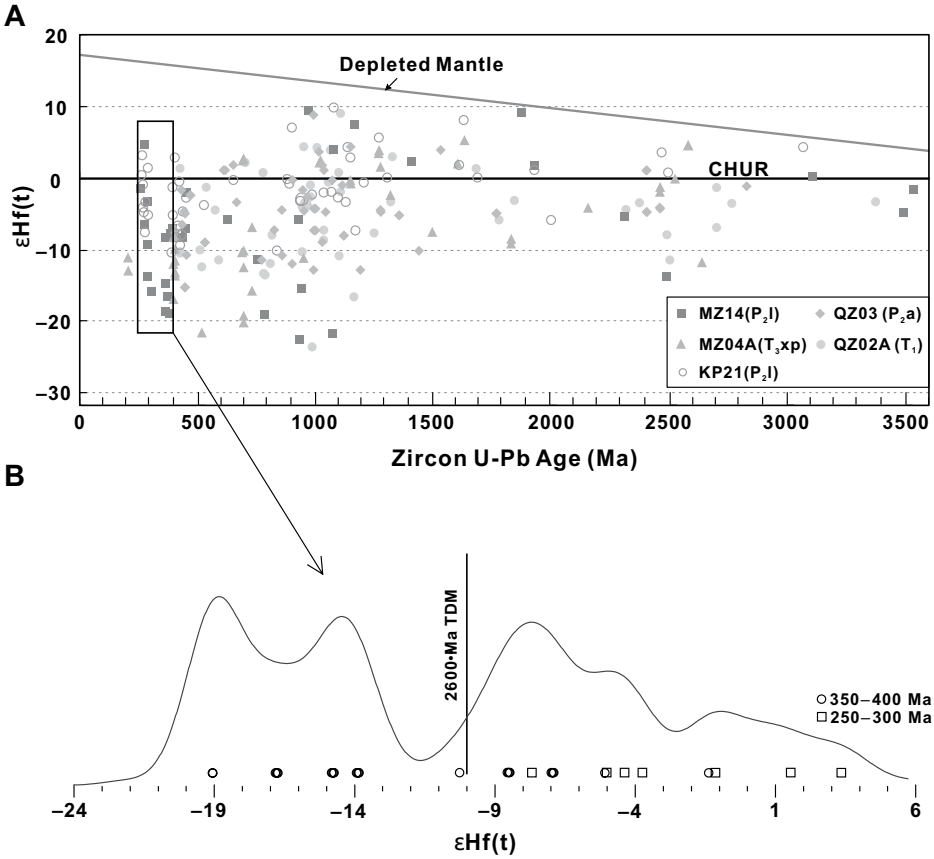

Figure 8. (A) Plot of $\varepsilon_{Hf}(t)$ vs. U-Pb ages for the detrital zircon grains from this study. Hf-isotope evolution line for depleted mantle follows Griffin et al. (2000). CHUR—chondritic uniform reservoir. (B) Kernel density estimation (KDE) of $\varepsilon_{Hf}(t)$ values from the 400–250 Ma zircon grains displaying mostly subchondritic $\varepsilon_{Hf}(t)$ values. TDM—depleted mantle model age. See Figure 3 caption for unit abbreviations.

with these ages could also have undergone multiple cycles from the former sedimentary successions because numerous zircon grains of this age have been reported in early Paleozoic sediments in the Yangtze and Cathaysia blocks (e.g., Wang et al., 2010). The late Mesoproterozoic to early Neoproterozoic detrital zircon grains (1190–940 Ma) with an age peak at ca. 956 Ma are abundant in all the study samples, especially in those of the Shiwandashan Basin (Meizhou: ~14.2%; Kaiping: ~22.9%; Qinzhou: ~31.5%; Figs. 7 and 9). Based on the sedimentary records and seismological and magnetotelluric sounding profiles through the Shiwandashan Basin, Liang and Li (2005) and X.C. Zhang et al. (2018) argued that Yunkai Mountain must have been emergent since the Late Permian or Middle Devonian, respectively. Thus, the presence of abundant 1190–940 Ma zircon grains in the former sedimentary units (e.g., Devonian and older) in the Yunkai Domain (e.g., Zhang et al., 2018) could ideally have acted as a nearby source to supply zircon grains with these ages to the Qinzhou area, as well as to the Kaiping area (Fig. 1C). Moreover, the late Mesoproterozoic to early Neoproterozoic magmatic rocks sporadically exposed in the Wuyi Domain of the Cathaysia block and in the Ailaoshan–Song Ma tectonic zone, and the Neoproterozoic to early Paleozoic sedimentary successions in the South China block (Wang et al., 2010; Usuki et al., 2013; Shu et al., 2015) could also have acted as potential sources to supply materials of this age. Late Neoproterozoic to early Paleozoic (650–500 Ma) zircon grains occur in all the studied samples (Figs. 7 and 9). However, igneous rocks with an age of 650–500 Ma, comparable with the timing of the Pan-African event in east Gondwanaland (Cawood et al., 2013), are not known to exist in the South China block. Thus, they are most likely sourced from the reworking of older sedimentary units, such as the early Paleozoic sedimentary rocks in the Cathaysia block (Wang et al., 2010; Xu et al., 2014) and the southwestern margin of the Yangtze block along the Ailaoshan–Song Ma tectonic zone (Wang et al., 2014). The Kwangsian (also named "Caledonian"; ca. 460–400 Ma) detrital zircon grains are ubiquitous in all the studied samples (accounting for ~11.5%–27.1%). These zircon grains usually display subhedral to enhedral crystal form, indicating short transport from their source area(s) (Fig. 5). The Kwangsian granitic rocks (mostly dated at 450–420 Ma), which are widely distributed in southeastern China to the eastern part of the Jiangnan Domain, could constitute the likely source (Fig. 1C; Chen and Jahn, 1998; Charvet et al., 1996, 2010; Wan et al., 2010; Li et al., 2010; Wang et al., 2007a).

In summary, 417 zircon grains from eight sandstone samples in the South China block yield a wide range of U-Pb ages from Archean (ca. 3500 Ma) to Mesozoic (ca. 205 Ma). Igneous rocks and multicycled sediments in the Wuyi-Yunkai Domains, Hainan Island, and the Jinshajiang–Ailaoshan–Song Ma orogenic belt are all likely sources for these pre–Middle Devonian zircon grains in the analyzed samples. The dominant Neoproterozoic cluster (990–960 Ma) of detrital zircon grains in the Shiwandashan Basin, together with the NW-NNW paleocurrent directions preserved in the Upper Permian to Middle Triassic strata (Liang and Li, 2005), argues that Yunkai Mountain should have been the major source for the detritus in the Shiwandashan foreland basin. Paleoproterozoic igneous rocks (ca. 2000–1600 Ma), mainly located in the NW Fujian and SW Zhejiang Provinces, provided more materials to the adjacent Meizhou, Yongding, and Yong'an Basins than the distal Kaiping area (Figs. 7 and 9).

Sources of the Post–Early Devonian Igneous Zircon Grains: Did Two Magmatic Events (400–350 Ma and 300–260 Ma) Occur in East Asia?

The post–Early Devonian detrital zircon grains in the samples from Kaiping and Meizhou commonly show three age clusters at 400–350 Ma, 300–260 Ma, and 257–205 Ma, while these ages are rare/absent in the samples from the Shiwandashan Basin (including the Qinzhou area; Figs. 7 and 9). Yunkai Mountain, which is adjacent to the Qinzhou area, may be the reason that there are rare younger materials (<400 Ma) in the Shiwandashan Basin. Abundant >400 Ma materials eroded from the Yunkai Mountain would dilute the proportion of the young materials (<400 Ma).

The proportion of 400–350 Ma zircon grains, with an age peak at ca. 380 Ma, accounts for ~10.5%–12.1% and ~6.1% in the Upper Permian–Upper Triassic samples in Meizhou and the Upper Permian sample in Kaiping, re-

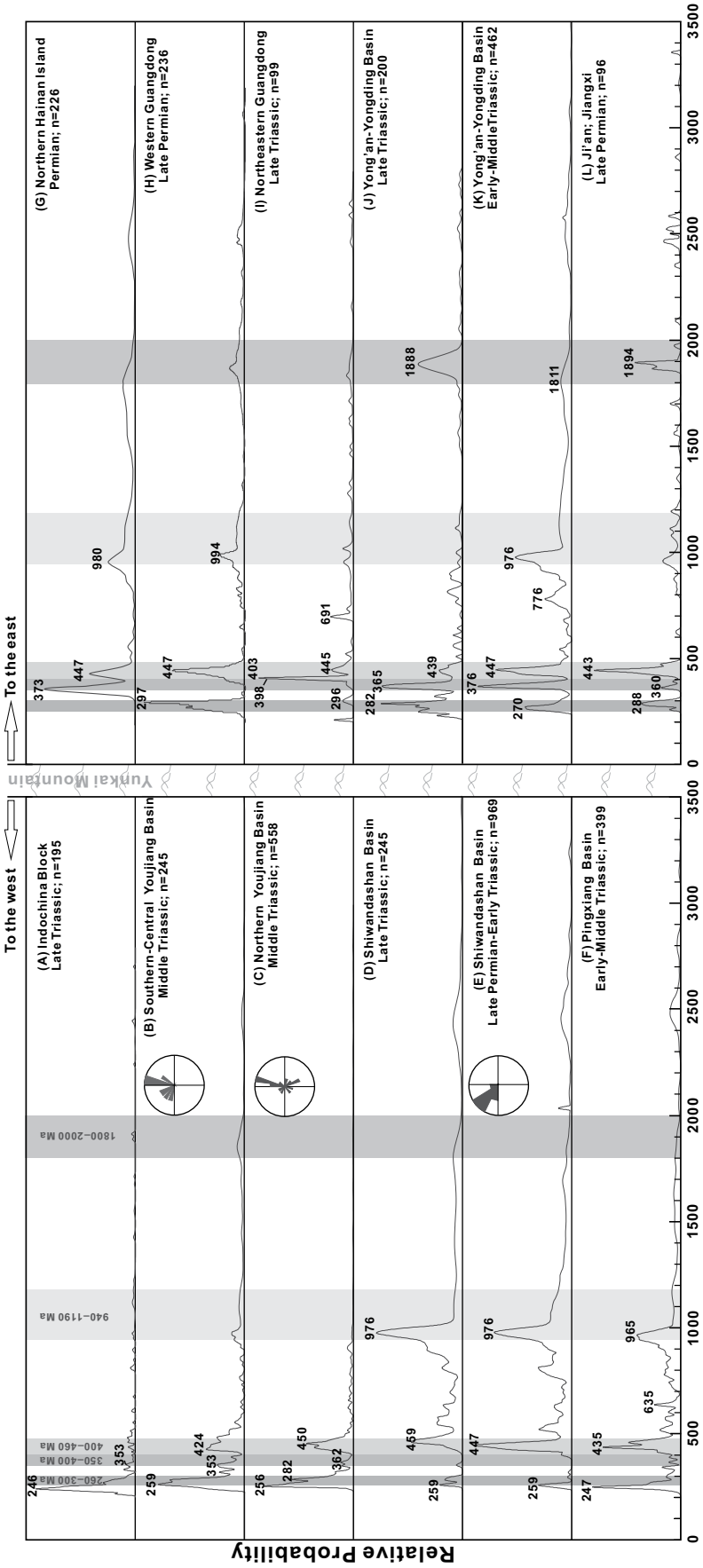

Figure 9. Summary of detrital zircon age distributions of sedimentary rocks from this study and other published literature. To the west of Yunkai Mountain: (A) Late Triassic samples from Thailand, central Laos, and central Vietnam in the Indochina block (Yan et al., 2017); (B–C) Middle Triassic samples from the Youjiang Basin (Yang et al., 2012; Yang and He, 2012), with rosette diagrams showing the paleocurrent directions; (D–E) Late Permian–Late Triassic samples from Shiwandashan Basin (Liang et al., 2013; Hu et al., 2014, 2015a; this study); (F) Early–Middle Triassic samples from Pingxiang Basin (Hu et al., 2017). To the east of Yunkai Mountain: (G) Permian samples from Hainan Island (L.M. Zhang et al., 2017); (H) Late Permian samples from western Guangdong Province (X.H. Li et al., 2012; Liang et al., 2013; this study); (I) Late Triassic samples from the Meizhou area, southeastern Guangdong Province, adjacent to the limited late Paleoproterozoic outcrops in the South China block (this study); (J–K) Triassic samples from Yong'an and Yongding basins in Fujian Province (Wang et al., 2009; X.H. Li et al., 2012; Liang et al., 2013; Hu et al., 2015a); (L) Late Permian samples from Ji'an, Jiangxi Province (X.H. Li et al., 2012). Important age peaks are shown with gray bands.

spectively. However, there are no rocks of this age identified in the South China block except for a few reports of granite with ages of 380–360 Ma in Hainan Island (Fu and Zhao, 1997; Ding et al., 2005). Thus, the sources of the 400–350 Ma zircon grains are enigmatic and debatable. X.H. Li et al. (2012) proposed that these grains in the Late Permian strata of the Yongding Basin were sourced from local crustal uplifts due to the "Huinan Movement," which was first mentioned by BGMRFJ (1985). Hu et al. (2015b, 2017) thought that these grains could have been derived from ca. 380–340 Ma metamorphic rocks in the South Kitakami belt of Japan (Isozaki et al., 2010), which was likely one segment of the South China block in the late Paleozoic to early Mesozoic. Moreover, on the basis of paleocurrents, Duan et al. (2018) argued that the 400–350 Ma and the 300–260 Ma zircon grains in the Middle Triassic strata in the Youjiang Basin may have originated from a now-missing magmatic source terrane near the southeastern South China block, which was formed by the subduction of the Paleo-Pacific plate beneath the Cathaysian margin of South China since the early Paleozoic. However, it is well known that the Paleo-Pacific was a huge ocean, which indicates that the related magmatic arc was formed in the framework of large-scale plate subduction. So, it is hard to imagine that there are no relict 400–350 Ma and 300–260 Ma rocks in southeastern China today. Furthermore, in the Middle Triassic, there were already many uplifted areas in the South China block that could be potential sources for the detritus in the Youjiang Basin, such as the Wuyi-Yunkai Domains in the western Cathaysia block (Fig. 1; Liang and Li, 2005; Li and Li, 2007; Hu et al., 2015b; Zhang et al., 2018). Thus, the source of sediments in Youjiang Basin would be diverse. Accordingly, simply using the paleocurrents to trace the provenance of the Late Permian–Triassic sediments through a complex geological background is inappropriate. Moreover, the interpretations above were mainly based on the following lines of evidence: (1) The west part of the Jiangnan orogen was mainly covered by carbonate during the Permian–Early Triassic, and thus would not have constituted an exposed source, and (2) outcrops of rocks with these ages on Hainan Island are extremely limited and unlikely to have provided abundant 400–350 Ma detrital zircon grains in the analyzed samples (X.H. Li et al., 2012; Hu et al., 2015b; Duan et al., 2018). However, recent studies have pointed out that there are indeed abundant 400–350 Ma detrital zircon grains in Permian strata on Hainan Island (L.M. Zhang et al., 2017; Hu et al., 2017). The long columnar and euhedral crystal forms of these zircon grains indicate that Hainan Island could have acted as a nearby source to supply zircon grains with these ages to northern Hainan Island (L.M. Zhang et al., 2017) and even to the South China block hinterland, such as the Meizhou, Yong'an, and Yongding Basins. Moreover, grains with these ages not only occur in the sedimentary deposits in the Cathaysia block, but they also can be found in the Middle Triassic strata in Youjiang Basin (Yang et al., 2012; Yang and He, 2012; Duan et al., 2018), the Paleozoic strata near the west side of the Ailaoshan belt (Wang et al., 2014), the Wuliangshan Group in the western Simao block (Xing et al., 2016), and modern river sediments of SE Asia in Indochina (monazite—Yokoyama et al., 2010; zircon—Bodet and Schärer, 2000). Therefore, the widespread detrital zircon grains of 400–350 Ma age in the southern South China block and its peripherals (Table 1) indicate a regional magmatic event rather than only a local crustal uplift near the Fujian Province (Table 1; Fig. 9). However, this uplift cannot be precluded for some samples in the Yong'an and Yongding Basins and southeast Guangdong Province usually have a relatively higher proportion of 400–350 Ma zircon grains than those from the Youjiang, Shiwandashan, Pingxiang, and Kaiping areas (Figs. 7 and 9).

Considering rare zircon grains of this age can be found in the Late Triassic Songpan-Ganzi complex (~5% in abundance; Weislogel et al., 2006) or in Paleogene strata of the Sichuan Basin (~3.8% in abundance; Jiang et al., 2013), and no eastward paleocurrents are preserved in Middle Triassic strata of the Youjiang Basin (Yang et al., 2012; Duan et al., 2018), we argue that the Songpan-Ganzi orogenic belt, located in the western part of the South China block, could not be the source. This speculation can be further supported by the fact that no coeval rocks are found in the Songpan-Ganzi orogenic belt. In addition, to the north, the North China block collided with the South China block during the Late Triassic (ca. 220–210 Ma; Li et al., 1993; Metcalfe, 2013), and so it also was not a possible source for the 400–350 Ma or 300–260 Ma zircon grains in this study. This can be further supported by the small proportion of the 2.6–2.4 Ga age group in the Permian–Triassic samples in the southern South China block (Fig. 7), whereas this is a characteristic age peak for the North China block (Diwu et al., 2008; Zheng et al., 2013). Instead, there are widespread magmatic rocks of this age along the Ailaoshan–Song Ma–Bangxi–Chenxing tectonic zone, including granites and mafic rocks with an age ranging from 387 to 340 Ma in the Jinshajiang–Ailaoshan–Song Ma tectonic zone (LA-ICP-MS zircon, 365–351 Ma—Lai et al., 2014a; sensitive high-resolution ion microprobe [SHRIMP] zircon, 383–376 Ma—Jian et al., 2009a; Sm-Nd whole rock, 387 Ma—Vượng et al., 2013), rhyolite dated at 374 Ma in the northern part of the Central Thailand volcanic belt (Intasopa and Dunn, 1994), tuffaceous chert within the Late Devonian strata of the Inthanon zone of northern Thailand (Hara et al., 2010), Late Devonian tholeiitic volcanics and early Carboniferous alkali basalts in the south margin of Youjiang Basin (Guo et al., 2004), and tuff yielding ages of 380–360 Ma within the Late Devonian volcanogenic sediments of the southern Lancangjiang zone in western Yunnan Province (Table 1; Nie et al., 2016). These rocks, together with the significant northward decrease in the amount of volcanic lithic fragments and 400–350 Ma detrital zircon grains, and the north-northeastward paleocurrents preserved in the Middle Triassic strata in the Youjiang Basin (Yang et al., 2012; Liang et al., 2013) suggest that there should be a Middle–Late Devonian igneous belt on the south margin of the South China block or its southern peripheral blocks that supplied detritus of this age to the entire southern South China block.

Although ages of 400–350 Ma have been widely recorded in Late Permian to Late Triassic sediments in the South China block, the origin of the coeval source rocks is still obscure. Some researchers thought that they may reflect a continuous lithospheric thinning event resulting from asthenosphere-lithosphere interaction within the South China block (Guo et al., 2004), or they were the result of a thermal effect from deep thermodynamics during the disintegration of Gondwana (Ding et al., 2005), while others have proposed that they represent a continuation of Late Ordovician–Late Silurian "Proto-Tethyan" subduction or the initial subduction stage of the Paleotethyan Ocean that occurred in the Late Devonian (Hara et al., 2010; Nie et al., 2016). Because rare volcanoes have been reported from the Sibumasu and Indochina blocks in northern Thailand during the Late Devonian–early Carboniferous, it is possible that such a volcano existed but has been mostly eroded away or covered by sedimentary rocks (Hara et al., 2010). In this study, the 400–350 Ma zircon grains have only subchondritic $\varepsilon_{Hf}(t)$ values of –19.1 to –1.4 with T_{DM}^{C} model ages from 1.48 to 2.58 Ga, implying that they were produced by Precambrian rocks and had almost no juvenile mantle material incorporated (Fig. 8B). Therefore, although further work is required to resolve the origin of these rocks, the tectonic settings of intraoceanic rifting can be ruled out.

In addition, there is another significant age group ranging from 300 to 260 Ma in Late

TABLE 1. GEOCHRONOLOGICAL DATA FROM MIDDLE–LATE DEVONIAN AND EARLY PERMIAN ZIRCON-BEARING INTERMEDIATE TO ACIDIC IGNEOUS ROCKS OR DETRITAL ZIRCONS FROM THE SOUTHERN MARGIN OF THE SOUTH CHINA BLOCK (SCB) AND SOUTHEAST ASIA

Location	Sample name	Lithology	Age (Ma)	Method*	Reference
Jinshajiang–Ailaoshan–Song Ma–Hainan suture zone					
Hainan	HN-16/3	Felsic gneiss	370.0 ± 4.4	SHRIMP zircon	Ding et al. (2005)
Hainan	JD-1	Felsic gneiss	362.9 ± 7.0	SHRIMP zircon	Ding et al. (2005)
Hainan	Baomeiling	Biotite moyite	369 ± 2. 9	Single zircon	Fu and Zhao (1997)
Western Ailaoshan	K09-16B	Plagiogranite	365 ± 7	LA-ICP-MS zircon	Lai et al. (2014a)
Western Ailaoshan	K09-16C	Plagiogranite	351 ± 11	LA-ICP-MS zircon	Lai et al. (2014a)
Western Simao block	WQ-1,MQ-17,MB-2	Tuff	378 ± 4, 366 ± 5, 382 ± 8	LA-ICP-MS zircon	Nie et al. (2016)
Western Simao block	WQ-7,MB-17	Upper Devonian sandstone	360–380	LA-ICP-MS zircon	Nie et al. (2016)
Western Simao block	09YN	Sandstone	~365	LA-ICP-MS zircon	Xing et al. (2016)
Western Ailaoshan	D01,C01,C02	Devonian–Carboniferous sandstone	~386	LA-ICP-MS zircon	Wang et al. (2014)
Hainan	11HN-07,19,23,45	Permian sandstone	370–380 (major)	LA-ICP-MS zircon	L.M. Zhang et al. (2017)
Hainan	15LJ15,49	Permian siltstone	360–400 (major)	LA-ICP-MS zircon	Hu et al. (2017)
Pingxiang (SCB)	PX20	Mid-Triassic sandstone	360–400	LA-ICP-MS zircon	Hu et al. (2017)
Hainan		Granite	267–272	SHRIMP zircon	Li et al. (2006)
Hainan		Shoshonitic intrusion	272 ± 7	SHRIMP zircon	Xie et al. (2006)
Hainan	Wuzhishan	Granitic gneisses	263~269	LA-ICP-MS zircon	Chen et al. (2011)
Yaxuanqiao	20SM-30	Volcanic rocks	265 ± 7	SHRIMP zircon	Fan et al. (2010)
Yaxuanqiao	20SM-33	Volcanic rocks	265 ± 7	SHRIMP zircon	Fan et al. (2010)
Dalongkai	ML18A	Plagioclase-pyroxenite	272 ± 2	LA-ICP-MS zircon	Liu et al. (2017)
Dalongkai	ML18E	Plagioclase	272 ± 2	LA-ICP-MS zircon	Liu et al. (2017)
Xuedui		Plagiogranite	294 ± 4	SHRIMP zircon	Wang et al. (2000)
Jiyidu	002-1	Granodiorite	263 ± 6	SHRIMP zircon	Jian et al. (2008)
Liangjiuding	007-4	Trondhjemite vein	285 ± 6	SHRIMP zircon	Jian et al. (2008)
Jiyidu	SJ-101	Tonalite	283 ± 3	SHRIMP zircon	Zi et al. (2012)
Baliu (Western Ailaoshan)	K10-56	Rhyolitic volcaniclastics	289 ± 3	LA-ICP-MS zircon	Lai et al. (2014b)
Chieng Khuong		Diorite	280–270	LA-ICP-MS zircon	Liu et al. (2012)
Southeast Asia					
Loei	PL 12-2	Breccia	359 ± 6	LA-ICP-MS zircon	Zaw and Meffre (2007)
Chiang Mai		Tuffaceous chert	350–400		Hara et al. (2010)
Loei	LV-14	Tuff	350 ± 2	LA-ICP-MS zircon	Qian et al. (2015)
Central Thailand		Rhyolite	374		Intasopa and Dunn (1994)
Modern river sediments			350–400	Monazite	Yokoyama et al. (2010);
Modern river sediments			350–400	Zircon	Bodet and Schärer (2000)
Bentong-Raub	106	Granodiorite	267 ± 2	Single zircon U-Pb	Liew and McCulloch (1985)
Jinghong	JI-7	Granodiorite intrusions	284 ± 1	LA-ICP-MS zircon	Hennig et al. (2009)
Jinghong	JI-56	Granodiorite intrusions	282 ± 1	LA-ICP-MS zircon	Hennig et al. (2009)
Sukhothai	MY53	Granite	266 ± 2	SIMS zircon	Gardiner et al. (2016)

*SHRIMP—sensitive high-resolution ion microprobe; LA-ICP-MS—laser ablation–inductively coupled plasma–mass spectrometry; SIMS—secondary ion mass spectrometry.

Permian–Late Triassic sandstones from Guangdong and Fujian Provinces (X.H. Li et al., 2012; Liang et al., 2013; Hu et al., 2015b; this study), Middle Triassic strata of the Youjiang Basin (Yang et al., 2012; Yang and He, 2012; Duan et al., 2018), Late Triassic strata of the Shiwandashan Basin (Hu et al., 2014), and post–Middle Triassic sediments of the Wuliangshan Group (where the youngest zircon age is ca. 259 Ma; Xing et al., 2016). These detrital zircon grains are generally euhedral to subhedral, suggesting short transport from their sources. However, in the same way, late Paleozoic igneous rocks are limited in the South China block and are only known from ca. 290–260 Ma potassic to calc-alkaline intrusive rocks in Hainan Island (Li et al., 2006; Xie et al., 2006; Chen et al., 2011). In contrast, outboard of the South China block, large numbers of igneous rocks yielding ages varying from ca. 300 to 260 Ma have been reported in the Jinshajiang–Ailaoshan–Song Ma suture zone, such as the Jiyidu tonalite (283 ± 3 Ma) from the Jinshajiang zone, the Baliu rhyolitic ignimbrite (289 ± 3 Ma) from the Ailaoshan zone, and the Chieng Khuong diorite (ca. 280 Ma) from the Song Ma zone (Table 1; Liew and McCulloch, 1985; Hennig et al., 2009; Jian et al., 2009a, 2009b; Maluski et al., 2005; Fan et al., 2010; Chen et al., 2011; Lai et al., 2014b; Gardiner et al., 2016; Wang et al., 2018). In addition, Hennig et al. (2009) reported some Jinghong granodiorite intrusions with a U-Pb zircon age of 284–282 Ma in the southern Lancangjiang zone (Table 1). The chemical and isotope signatures show that these granodiorite intrusions formed in an arc setting (Hennig et al., 2009). Wang et al. (2018) also pointed out magmatism with arc and back-arc geochemical signatures along the Jinshajiang–Ailaoshan–Song Ma, Wusu, and Truong Son suture zones, mainly dated at 289–260 Ma. In SE Asia, these rocks originated from the opening and closure of the Jinshajiang–Ailaoshan–Song Ma back-arc basin/branch ocean, which formed at ca. 439–374 Ma and finally closed at ca. 247 Ma (Hennig et al., 2009; Jian et al., 2009a, 2009b; Fan et al., 2010; Liu et al., 2012, 2015, 2017; Vượng et al., 2013; Wang et al., 2013), or they were related to closure of the main East Paleotethyan Ocean, which opened in the Middle–Late Devonian to earliest Carboniferous and finally closed during the Triassic (Fan et al., 2010; Wang et al., 2018). These rocks, together with outcrops on Hainan Island, are all potential sources that could have supplied coeval detritus to the South China block hinterland, lending support to the provenance interpretation of the Late Devonian–Carboniferous detrital zircon grains. Moreover, considering that the 300–260 Ma and 400–350 Ma age groups have been found in the Late Permian Longtan Formation (P_2l) in the Kaiping and Meizhou sections (Figs. 1, 7A, 7E, and 7F) and considering the oblique convergence of the Jinshajiang–Ailaoshan–Song Ma–Chenxing back-arc basin/branch ocean (Carter and Clift, 2008; Hu et al., 2015b), we propose that the South China block and the Indochina block may have welded together during the Late Permian (e.g., Chen et al., 2011) near Hainan Island, facilitating the transport of these materials northward to the South China block hinterland. Alternatively, zircon grains with these ages could have been floated to the South China block in the form of volcanic ash, or perhaps the back-arc basin/branch ocean was not broad enough to prevent them from being transported northward to the South China block. In any case,

all this evidence strongly indicates that there were two magmatic events (400–350 Ma and 300–260 Ma) in East Asia, either within or beyond the southern margin of the South China block, that acted as the potential sources for the Permian–Triassic sediments in the southern South China block hinterland.

Tectonic Implications of the South China Block During the Indosinian Period

The provenance analysis herein has shown that there should be two magmatic belts that wrapped around the southern South China block to supply materials northward, but this interpretation does not match with the Paleo-Pacific subduction model, which is based on the assumption that the active continental margin of the South China block existed since the earliest Permian (ca. 280 Ma; Fig. 2C; e.g., Li and Li, 2007; X.H. Li et al., 2006, 2012; Z.X. Li et al., 2012). Accordingly, an alternative provenance interpretation has been proposed involving derivation from the active continental margin of the southeastern coast of China and/or even from Japan (X.H. Li et al., 2006, 2012; Z.X. Li et al., 2012; Li and Li, 2007; Zhu et al., 2014; Pang et al., 2014; Hu et al., 2015b; Jiang et al., 2015). Using sediment records (Fig. 1C), Hu et al. (2014, 2015a, 2015b, 2017) further hypothesized that the South China block could be divided into western and eastern parts by Yunkai Mountain. In this model, the late Paleozoic to early Mesozoic sedimentation in the Youjiang-Shiwandashan Basins to the west of Yunkai Mountain was affected by the Paleotethys tectonic zone, while that in the Yong'an Basin to the east of Yunkai Mountain was under the influence of the Paleo-Pacific tectonic zone.

The onset of Paleo-Pacific subduction is still controversial, ranging from the Devonian to Early–Middle Jurassic (Taylor and Hayes, 1983; Engebretson et al., 1985; Zhou and Li, 2000; Li and Li, 2007; Carter and Clift, 2008; X.H. Li et al., 2012; Hennig et al., 2017; Breitfeld et al., 2017; Duan et al., 2018). Although it is difficult to judge when the Paleo-Pacific subduction started, the earliest Permian subduction of the Paleo-Pacific model need explain the following: (1) SE-dipping thrusting, synorogenic magmatism, and foreland basin deposition did not propagate toward the cratonic interior in response to developing flat-slab subduction of the Paleo-Pacific Ocean plate (Faure et al., 1996; Chen, 1999; Yan et al., 2003; Wang et al., 2005, 2007b, 2013; Zhang et al., 2013; Shu et al., 2015), and (2) late Paleozoic to early Mesozoic arc magmatism is not recognized in the South China block (X.H. Li et al., 2012; Hu et al., 2015b, 2017; Duan et al., 2018).

Sedimentary sequences record significant information on their depositional environment and tectonic setting, and they can be used as a proxy for constraining "source-to-sink" processes (e.g., X.C. Zhang et al., 2017; Hennig et al., 2018). In this study, our data show that the U-Pb age spectra of detrital zircon grains in the Late Permian to Late Triassic sandstones in the South China block are chaotic (Figs. 7 and 9). For example, sediments in the Shiwandashan Basin usually contain a small amount of late Paleozoic detrital zircon grains, while they are ubiquitous in the Youjiang Basin and in the southeastern South China block (Figs. 7 and 9). Moreover, sandstones in the South China block do not show a tendency for maturation westward (Fig. 4). The Late Permian to Triassic sandstone in the Meizhou section is quartzose sandstone, while those in the Shiwandashan Basin and the Kaiping section are mainly graywacke (Fig. 4). This information, together with the SW-NE trend of fining grain size in Shiwandashan Basin in Guangxi Province and Yong'an Basin in Fujian Province (Liang et al., 2013), indicates there may be a process of conveying sediments from south to north. These constraints further demonstrate that sediments in the southern South China block should be partly sourced from areas within or beyond the southern margin of the South China block. Thus, our new data, together with published data from the southern South China block, show that the Late Permian–Triassic sedimentation in the southern South China block was most likely affected by the evolution of the East Paleotethyan Ocean and even the Proto-Tethyan Ocean, and by the closure of the Jinshajiang–Ailaoshan–Song Ma back-arc basin/branch ocean. This information, together with the large-scale positive flower structure in South China, suggests that the Indosinian orogenesis in South China was most likely caused by far-field effects of subduction/collision processes along the boundary of South China, e.g., the North China–South China and Indochina–South China collision (Figs. 2A, 2B, and 10; e.g., Faure et al., 2016; Charvet et al., 2010; Wang et al., 2007a, 2007b, 2013; Shu et al., 2008, 2009, 2015).

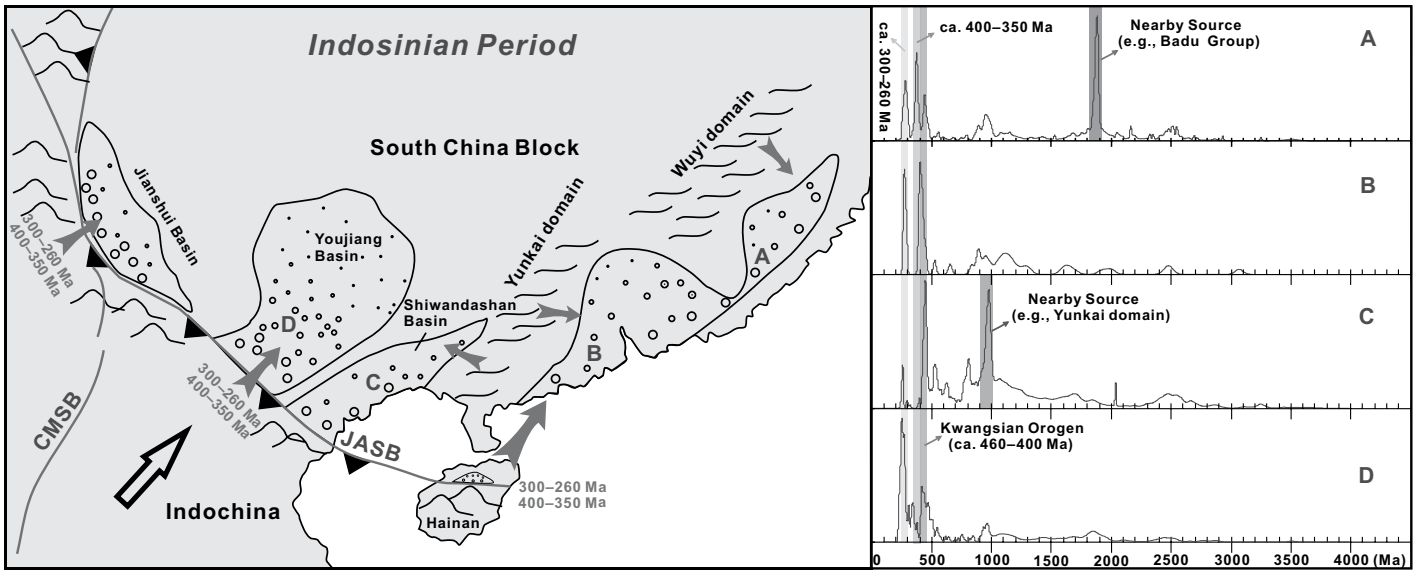

Figure 10. Schematic cartoon depicting the sources of Late Permian–Triassic strata of the South China block, where solid black arrows indicate paleotransport directions. JASB—Jinshajiang–Ailaoshan–Song Ma belt; CMSB—Changning-Menglian and Chiangmai suture zone.

CONCLUSIONS

Petrographic analysis and detrital zircon U-Pb geochronology show that the Late Permian to Late Triassic sediments in the overlapping area of the Paleotethys and Paleo-Pacific tectonic zones were mainly derived from the Wuyi-Yunkai Domains of the Cathaysia block, as well as some potential rocks with ages of 400–350 Ma and 300–260 Ma. Detrital zircon grains with ages of 400–350 Ma and 300–260 Ma are ubiquitous around the southern margin of the South China block, but nonexistent or rare coeval igneous rocks in the South China block indicate that these age groups define two igneous events developed in East Asia, either within or beyond the southern margin of the South China block. The 400–350 Ma zircon grains have subchondritic $\varepsilon_{Hf}(t)$ values of –19.1 to –1.4 with T_{DM}^{C} model ages from 1.48 to 2.58 Ga, implying that these rocks did not form in settings of intraoceanic rifting, but may be associated with the evolution of the Tethyan Ocean. The origin of 300–260 Ma rocks was most likely related to the subduction and closure of the main East Paleotethyan Ocean or the Jinshajiang–Ailaoshan–Song Ma–Hainan back-arc basin/branch ocean, because these rocks show arc-like geochemical signatures. These age features in combination with the petrographic analysis and other evidence suggest that the Late Permian to Triassic sediments in the South China block were partly sourced from these two igneous belts within or beyond the southern South China block, rather than from rocks in the southeast China. Our new data lend support to the idea that the Indosinian orogeny in the South China block was most likely triggered by continental collisions. Meanwhile, sedimentation in the southern South China block was largely affected by the evolution of Tethys and not the Paleo-Pacific.

ACKNOWLEDGMENTS

We are grateful to Science Editor Rob Strachan, Associate Editor Anna Bird, Juliane Hennig-Breitfeld, and one anonymous reviewer for their constructive reviews and insightful suggestions. We would like to thank Qingli Tan for his assistance in the field work. The data for this paper are available as Data Repository Tables S1–S3 (see footnote 1). This work was jointly supported by the National Natural Science Foundation of China (grant 41602232 and U1701641), the National Key Research and Development Project of China (grant 2016YFC0600303), and the National Basic Research Program of China (grant 2014CB440901). This is contribution No. IS-2618 from GIGCAS.

REFERENCES CITED

Blichert-Toft, J., Chauvel, C., and Albarede, F., 1997, Separation of Hf and Lu for high-precision isotope analysis of rock samples by magnetic sector multiple collector ICP-MS: Contributions to Mineralogy and Petrology, v. 127, p. 248–260, https://doi.org/10.1007/s004100050278.

Bodet, F., and Schärer, U., 2000, Evolution of the SE-Asian continent from U-Pb and Hf isotopes in single grains of zircon and baddeleyite from large rivers: Geochimica et Cosmochimica Acta, v. 64, p. 2067–2091, https://doi.org/10.1016/S0016-7037(00)00352-5.

Breitfeld, H.T., Hall, R., Galin, T., Forster, M.A., and Bou-Dagher-Fadel, M.K., 2017, Triassic to Cretaceous Sundaland–Pacific subduction margin in West Sarawak, Borneo: Tectonophysics, v. 694, p. 35–56, https://doi.org/10.1016/j.tecto.2016.11.034.

Breitfeld, H.T., Hall, R., Galin, T., and BouDagher-Fadel, M.K., 2018, Unravelling the stratigraphy and sedimentation history of the uppermost Cretaceous to Eocene sediments of the Kuching zone in West Sarawak (Malaysia), Borneo: Journal of Asian Earth Sciences, v. 160, p. 200–223, https://doi.org/10.1016/j.jseaes.2018.04.029.

Bureau of Geology and Mineral Resources of Fujian Province (BGMRFJ), 1985, Regional Geology of the Fujian Province: Beijing, Geology Publishing House, 671 p. [in Chinese with English summary].

Bureau of Geology and Mineral Resources of Guangdong Province (BGMRGD), 1988, Regional Geology of Guangdong Province: Beijing, Geology Publishing House, 971 p. [in Chinese with English summary].

Bureau of Geology and Mineral Resources of Guangxi Province (BGMRGX), 1985, Regional Geology of the Guangxi Province: Beijing, Geology Publishing House, 853 p. [in Chinese with English summary].

Carter, A., and Clift, P.D., 2008, Was the Indosinian orogeny a Triassic mountain building or a thermotectonic reactivation event?: Comptes Rendus Geoscience, v. 340, p. 83–93, https://doi.org/10.1016/j.crte.2007.08.011.

Carter, A., Roques, D., Bristow, C., and Kinny, P., 2001, Understanding Mesozoic accretion in Southeast Asia: Significance of Triassic thermotectonism (Indosinian orogeny) in Vietnam: Geology, v. 29, p. 211–214, https://doi.org/10.1130/0091-7613(2001)029<0211:UMAISA>2.0.CO;2.

Cawood, P.A., Wang, Y.J., Xu, Y.J., and Zhao, G.C., 2013, Locating South China in Rodinia and Gondwana: A fragment of greater India lithosphere?: Geology, v. 41, p. 903–906, https://doi.org/10.1130/G34395.1.

Charvet, J., Shu, L.S., Shi, Y.S., Guo, L.Z., and Faure, M., 1996, The building of South China: Collision of Yangtze and Cathaysia blocks, problems and tentative answers: Journal of Southeast Asian Earth Sciences, v. 13, p. 223–235, https://doi.org/10.1016/0743-9547(96)00029-3.

Charvet, J., Shu, L.S., Faure, M., Choulet, F., Wang, B., Lu, H.F., and Breton, N.L., 2010, Structural development of the Lower Paleozoic belt of South China: Genesis of an intracontinental orogeny: Journal of Asian Earth Sciences, v. 39, p. 309–330, https://doi.org/10.1016/j.jseaes.2010.03.006.

Chen, A., 1999, Mirror thrusting in the South China orogenic belt: Tectonic evidence from western Fujian, southeastern China: Tectonophysics, v. 305, p. 497–519, https://doi.org/10.1016/S0040-1951(99)00036-0.

Chen, J.F., and Jahn, B.M., 1998, Crustal evolution of southeastern China: Nd and Sr isotopic evidence: Tectonophysics, v. 284, p. 101–133, https://doi.org/10.1016/S0040-1951(97)00186-8.

Chen, X.Y., Wang, Y.J., Fan, W.M., Peng, T.P., Zhang, F.F., and Zhang, Y.Z., 2011, Zircon LA-ICP-MS U-Pb dating of granitic gneisses from Wuzhishan area, Hainan, and geological significances: Geochimica, v. 40, p. 454–463 [in Chinese with English abstract].

Dickinson, W.R., and Suczek, C.A., 1979, Plate tectonics and sandstone compositions: American Association of Petroleum Geologists Bulletin, v. 63, p. 2164–2182.

Ding, S.J., Hu, J.M., Song, B., Chen, M.L., Xie, S.Z., and Fan, Y., 2005, U-Pb dating of zircon from the bed parallel anatectic granitic intrusion in the Baoban group in Hainan Island and the tectonic implication: Science in China, ser. D, Earth Sciences, v. 48, p. 2092–2103, https://doi.org/10.1360/04yd0039.

Diwu, C., Sun, Y., Yuan, H.L., Wang, H.L., Zhong, X.P., and Liu, X.M., 2008, U-Pb ages and Hf isotopes for detrital zircons from quartzite in the Paleoproterozoic Songshan Group on the southwestern margin of the North China craton: Chinese Science Bulletin, v. 53, no. 18, p. 2828–2839.

Duan, L., Meng, Q.R., Christie-Blick, N., and Wu, G.L., 2018, New insights on the Triassic tectonic development of South China from the detrital zircon provenance of Nanpanjiang turbidites: Geological Society of America Bulletin, v. 130, p. 24–34, https://doi.org/10.1130/B31630.1.

Engebretson, D.C., Cox, A., and Gordon, R.G., 1985, Relative Motions Between Oceanic and Continental Plates in the Pacific Basins: Geological Society of America Special Paper 206, 59 p., https://doi.org/10.1130/SPE206-p1.

Fan, W.M., Wang, Y.J., Zhang, A.M., Zhang, F.F., and Zhang, Y.Z., 2010, Permian arc–back-arc basin development along the Ailaoshan tectonic zone: Geochemical, isotopic and geochronological evidence from the Mojiang volcanic rocks, southwest China: Lithos, v. 119, p. 553–568, https://doi.org/10.1016/j.lithos.2010.08.010.

Faure, M., Sun, Y., Shu, L., Monie, P., and Charvet, J., 1996, Extensional tectonics within a subduction-type orogeny. The case study of the Wugongshan dome (Jiangxi Province, southeastern China): Tectonophysics, v. 263, p. 77–106, https://doi.org/10.1016/S0040-1951(97)81487-4.

Faure, M., Lepvrier, C., Nguyen, V.V., Vu, V.T., Lin, W., and Chen, Z., 2014, The South China block–Indochina collision: Where, when, and how?: Journal of Asian Earth Sciences, v. 79, p. 260–274, https://doi.org/10.1016/j.jseaes.2013.09.022.

Faure, M., Lin, W., Chu, Y., and Lepvrier, C., 2016, Triassic tectonics of the Ailaoshan belt (SW China): Early Triassic collision between the South China and Indochina blocks, and Middle Triassic intracontinental shearing: Tectonophysics, v. 683, p. 27–42, https://doi.org/10.1016/j.tecto.2016.06.015.

Fu, J.M., and Zhao, Z.J., 1997, The characteristics and tectonic settings of Caledonian granite in Hainan Island: Journal of Mineral Petrology, v. 17, p. 29–34 [in Chinese with English abstract].

Gao, S., Ling, W.L., Qiu, Y., Zhou, L., Hartmann, G., and Simon, K., 1999, Contrasting geochemical and Sm-Nd isotopic compositions of Archean metasediments from the Kongling high-grade terrain of the Yangtze craton: Evidence for cratonic evolution and redistribution of REE during crustal anataxis: Geochimica et Cosmochimica Acta, v. 63, p. 2071–2088, https://doi.org/10.1016/S0016-7037(99)00153-2.

Gardiner, N.J., Searle, M.P., Morley, C.K., Whitehouse, M.P., Spencer, C.J., and Robb, L.J., 2016, The closure of Palaeotethys in eastern Myanmar and northern Thailand: New insights from zircon U-Pb and Hf isotope data: Gondwana Research, v. 39, p. 401–422, https://doi.org/10.1016/j.gr.2015.03.001.

Greentree, M.R., and Li, Z.X., 2008, The oldest known rocks in south-western China: SHRIMP U-Pb magmatic crystallisation age and detrital provenance analysis of the Paleoproterozoic Dahongshan Group: Journal of Asian Earth Sciences, v. 33, p. 289–302, https://doi.org/10.1016/j.jseaes.2008.01.001.

Griffin, W.L., Pearson, N.J., Belousova, E., Jackson, S.E., van Achterbergh, E., O'Reilly, S.Y., and Shee, S.R., 2000, The Hf isotope composition of cratonic mantle: LAM-MC-ICPMS analysis of zircon megacrysts in kimberlites: Geochimica et Cosmochimica Acta, v. 64, p. 133–147, https://doi.org/10.1016/S0016-7037(99)00343-9.

Griffin, W.L., Wang, X., Jackson, S.E., Pearson, N.J., O'Reilly, S.Y., Xu, X.S., and Zhou, X.M., 2002, Zircon chemistry and magma mixing, SE China: In-situ analysis of Hf isotopes, Tonglu and Pingtan igneous complexes: Lithos, v. 61, p. 237–269, https://doi.org/10.1016/S0024-4937(02)00082-8.

Griffin, W.L., Belousova, E.A., Shee, S.R., Pearson, N.J., and O'Reilly, S.Y., 2004, Archean crustal evolution in the northern Yilgarn craton: U-Pb and Hf isotope evidence from detrital zircons: Precambrian Research, v. 131, p. 231–282, https://doi.org/10.1016/j.precamres.2003.12.011.

Guo, F., Fan, W.M., Wang, Y.J., and Li, C.W., 2004, Upper Paleozoic basalts in the southern Yangtze block:

Geochemical and Sr-Nd isotopic evidence for asthenosphere-lithosphere interaction and opening of the Paleo-Tethyan Ocean: International Geology Review, v. 46, p. 332–346, https://doi.org/10.2747/0020-6814.46.4.332.

Hara, H., Kurihara, T., Kuroda, J., Adachi, Y., Kurita, H., Wakita, K., Hisada, K., Charusiri, P., Charoentitirat, T., and Chaodumrong, P., 2010, Geological and geochemical aspects of a Devonian siliceous succession in northern Thailand: Implications for the opening of the Paleo-Tethys: Palaeogeography, Palaeoclimatology, Palaeoecology, v. 297, p. 452–464, https://doi.org/10.1016/j.palaeo.2010.08.029.

Hara, H., Kunii, M., Hisada, K.I., Ueno, K., Kamata, Y., Srichan, W., Charusiri, P., Charoentitirat, T., Watarai, M., Adachi, Y., and Kurihara, T., 2012, Petrography and geochemistry of clastic rocks within the Inthanon zone, northern Thailand: Implications for paleo-Tethys subduction and convergence: Journal of Asian Earth Sciences, v. 61, p. 2–15, https://doi.org/10.1016/j.jseaes.2012.06.012.

Hennig, D., Lehmann, B., Frei, D., Belyatsky, B., Zhao, X.F., Cabral, A.R., Zeng, P.S., Zhou, M.F., and Schmidt, K., 2009, Early Permian seafloor to continental arc magmatism in the eastern Paleo-Tethys: U-Pb age and Nd-Sr isotope data from the southern Lancangjiang zone, Yunnan, China: Lithos, v. 113, p. 408–422, https://doi.org/10.1016/j.lithos.2009.04.031.

Hennig, J., Breitfeld, H.T., Hall, R., and Nugraha, A.M.S., 2017, The Mesozoic tectono-magmatic evolution at the Paleo-Pacific subduction zone in West Borneo: Gondwana Research, v. 48, p. 292–310, https://doi.org/10.1016/j.gr.2017.05.001.

Hennig, J., Breitfeld, H.T., Gough, A., Hall, R., Long, T.V., Kim, V.M., and Quang, S.D., 2018, U-PB zircon ages and provenance of Upper Cenozoic sediments from the Da Lat zone, SE Vietnam: Implications for an intra-Miocene unconformity and paleo-drainage of the proto–Mekong River: Journal of Sedimentary Research, v. 88, no. 4, p. 495–515, https://doi.org/10.2110/jsr.2018.26.

Hu, L.S., Du, Y.S., Cawood, P.A., Xu, Y.J., Yu, W.C., Zhu, Y.H., and Yang, J.H., 2014, Drivers for late Paleozoic to early Mesozoic orogenesis in South China: Constraints from the sedimentary record: Tectonophysics, v. 618, p. 107–120, https://doi.org/10.1016/j.tecto.2014.01.037.

Hu, L.S., Cawood, P.A., Du, Y.S., Xu, Y.J., Xu, W.C., and Huang, H.W., 2015a, Detrital records for Upper Permian–Lower Triassic succession in the Shiwandashan Basin, South China, and implication for Permo-Triassic (Indosinian) orogeny: Journal of Asian Earth Sciences, v. 98, p. 152–166, https://doi.org/10.1016/j.jseaes.2014.11.007.

Hu, L.S., Cawood, P.A., Yang, J.H., and Jiao, L.X., 2015b, Late Paleozoic to early Mesozoic provenance record of Paleo-Pacific subduction beneath South China: Tectonics, v. 34, p. 986–1008, https://doi.org/10.1002/2014TC003803.

Hu, L.S., Cawood, P.A., Du, Y.S., Xu, Y.J., Wang, C.H., Wang, Z.W., Ma, Q.L., and Xu, X.R., 2017, Permo-Triassic detrital records of South China and implications for the Indosinian events in East Asia: Palaeogeography, Palaeoclimatology, Palaeoecology, v. 485, p. 84–100, https://doi.org/10.1016/j.palaeo.2017.06.005.

Intasopa, S., and Dunn, T., 1994, Petrology and Sr-Nd isotopic systems of the basalts and rhyolites, Loei, Thailand: Journal of Southeast Asian Earth Sciences, v. 9, p. 167–180, https://doi.org/10.1016/0743-9547(94)90073-6.

Isozaki, Y.K., Nakama, A.T., and Yanai, S., 2010, New insight into a subduction-related orogen: A reappraisal of the geotectonic framework and evolution of the Japanese Islands: Gondwana Research, v. 18, p. 82–105, https://doi.org/10.1016/j.gr.2010.02.015.

Jian, P., Liu, D.Y., and Sun, X.M., 2008, SHRIMP dating of the Permo-Carboniferous Jinshajiang ophiolite, southwestern China: geochronological constraints for the evolution of Paleo-Tethys: Journal of Asian Earth Sciences, v. 32, p. 371–384.

Jian, P., Liu, D.Y., Kröner, A., Zhang, Q., Wang, Y.Z., Sun, X.M., and Zhang, W., 2009a, Devonian to Permian plate tectonic cycle of the Paleo-Tethys orogen in southwest China (I): Geochemistry of ophiolites, arc/back-arc assemblages and within-plate igneous rocks: Lithos, v. 113, p. 748–766, https://doi.org/10.1016/j.lithos.2009.04.004.

Jian, P., Liu, D.Y., Kröner, A., Zhang, Q., Wang, Y.Z., Sun, X.M., and Zhang, W., 2009b, Devonian to Permian plate tectonic cycle of the Paleo-Tethys orogen in southwest China (II): Insights from zircon ages of ophiolites, arc/back-arc assemblages and within-plate igneous rocks and generation of the Emeishan CFB province: Lithos, v. 113, p. 767–784, https://doi.org/10.1016/j.lithos.2009.04.006.

Jiang, X.Y., Li, X.H., Collin, W.J., and Huang, H.Q., 2015, U-Pb age and Hf-O isotopes of detrital zircons from Hainan Island: Implications for Mesozoic subduction models: Lithos, v. 239, p. 60–70, https://doi.org/10.1016/j.lithos.2015.10.006.

Jiang, Z.F., Wu, H., Cui, X.Z., Zhuo, J.W., and Jiang, X.S., 2013, Detrital zircon U-Pb geochronology of the Liujia Formation of Paleogene in Sichuan Basin and its geological significance: Journal of Mineralogy and Petrology, v. 33, p. 76–84 [in Chinese with an English abstract].

Lai, C.K., Meffre, S., Crawford, A.J., Zaw, K., Halpin, J.A., Xue, C.D., and Salam, A., 2014a, The Central Ailaoshan ophiolite and modern analogs: Gondwana Research, v. 26, p. 75–88, https://doi.org/10.1016/j.gr.2013.03.004.

Lai, C.K., Meffre, S., Crawford, A.J., Zaw, K., Xue, C.D., and Halpin, J.A., 2014b, The western Ailaoshan volcanic belts and their SE Asia connection: A new tectonic model for the eastern Indochina block: Gondwana Research, v. 26, p. 52–74, https://doi.org/10.1016/j.gr.2013.03.003.

Lepvrier, C., Maluski, H., Vuong, N.V., Roques, D., Axente, V., and Rangin, C., 1997, Indosinian NW-trending shear zones within the Truong Son belt (Vietnam): ^{40}Ar-^{39}Ar Triassic ages and Cretaceous to Cenozoic overprints: Tectonophysics, v. 283, p. 105–127, https://doi.org/10.1016/S0040-1951(97)00151-0.

Lepvrier, C., Maluski, H., Tich, V.V., Leyreloup, A., Thi, P.T., and Vuong, N.V., 2004, The early Triassic Indosinian orogeny in Vietnam (Truong Son belt and Kontum massif); implications for the geodynamic evolution of Indochina: Tectonophysics, v. 393, no. 1-4, p. 87–118, https://doi.org/10.1016/j.tecto.2004.07.030.

Lepvrier, C., Vuong, N.V., Maluski, H., Thi, P.T., and Vu, T.V., 2008, Indosinian tectonics in Vietnam: Comptes Rendus Geoscience, v. 340, p. 94–111, https://doi.org/10.1016/j.crte.2007.10.005.

Lepvrier, C., Faure, M., Vuong, N.V., Vu, T.V., Lin, W., Thang, T.T., Phuong, T.H., and Hoa, P.T., 2011, North-directed Triassic nappes in northeastern Vietnam (East Bac Bo): Journal of Asian Earth Sciences, v. 41, p. 56–68, https://doi.org/10.1016/j.jseaes.2011.01.002.

Li, S.G., Xiao, Y.L., Liu, D.L., Chen, Y.Z., Ge, N.J., Zhang, Z.Q., Sun, S.S., Cong, B.L., Zhang, R.Y., Hart, S.R., and Wang, S.S., 1993, Collision of the North China and Yangtze blocks and formation of coesite-bearing eclogites: Timing and processes: Chemical Geology, v. 109, p. 89–111, https://doi.org/10.1016/0009-2541(93)90063-O.

Li, X.H., Li, Z.X., Li, W.X., and Wang, Y.J., 2006, Initiation of the Indosinian orogeny in South China: Evidence for a Permian magmatic arc on Hainan Island: The Journal of Geology, v. 114, p. 341–353, https://doi.org/10.1086/501222.

Li, X.H., Li, W.X., Li, Z.X., Lo, C.H., Wang, J., Ye, M.F., and Yang, Y.H., 2009, Amalgamation between the Yangtze and Cathaysia blocks in South China: Constraints from SHRIMP U-Pb zircon ages, geochemistry and Nd-Hf isotopes of the Shuangxiwu volcanic rocks: Precambrian Research, v. 174, p. 117–128, https://doi.org/10.1016/j.precamres.2009.07.004.

Li, X.H., Li, Z.X., He, B., Li, W.X., Li, Q.L., Gao, Y.Y., and Wang, X.C., 2012, The Early Permian active continental margin and crustal growth of the Cathaysia block: In situ U-Pb, Lu-Hf and O isotope analyses of detrital zircons: Chemical Geology, v. 328, p. 195–207, https://doi.org/10.1016/j.chemgeo.2011.10.027.

Li, Z.X., and Li, X.H., 2007, Formation of the 1300-km-wide intracontinental orogen and postorogenic magmatic province in Mesozoic South China: A flat-slab subduction model: Geology, v. 35, p. 179–182, https://doi.org/10.1130/G23193A.1.

Li, Z.X., Li, X.H., Zhou, H.W., and Kinny, P.D., 2002, Grenvillian continental collision in south China: New SHRIMP U-Pb zircon results and implications for the configuration of Rodinia: Geology, v. 30, p. 163–166, https://doi.org/10.1130/0091-7613(2002)030<0163:GCCISC>2.0.CO;2.

Li, Z.X., Li, X.H., Li, W.X., and Ding, S.J., 2008, Was Cathaysia part of Proterozoic Laurentia?—New data from Hainan Island, South China: Terra Nova, v. 20, p. 154–164, https://doi.org/10.1111/j.1365-3121.2008.00802.x.

Li, Z.X., Li, X.H., Wartho, J.A., Clark, C., Li, W.X., Zhang, C.L., and Bao, C., 2010, Magmatic and metamorphic events during the early Paleozoic Wuyi-Yunkai orogeny, southeastern South China: New age constraints and pressure-temperature conditions: Geological Society of America Bulletin, v. 122, p. 772–793, https://doi.org/10.1130/B30021.1.

Li, Z.X., Li, X.H., Chung, S.L., Lo, C.H., Xu, X.S., and Li, W.X., 2012, Magmatic switch-on and switch-off along the South China continental margin since the Permian: Transition from an Andean-type to a western Pacific–type plate boundary: Tectonophysics, v. 532–535, p. 271–290, https://doi.org/10.1016/j.tecto.2012.02.011.

Liang, X.Q., and Li, X.H., 2005, Late Permian to Middle Triassic sedimentary records in Shiwandashan Basin: Implication for the Indosinian Yunkai orogenic belt, South China: Sedimentary Geology, v. 177, p. 297–320, https://doi.org/10.1016/j.sedgeo.2005.03.009.

Liang, X.Q., Zhou, Y., Jiang, Y., Wen, S.N., Fu, J.G., and Wang, C., 2013, Difference of sedimentary response to Dongwu movement: Study on LA-ICPMS U-Pb ages of detrital zircons from Upper Permian Wujiaping or Longtan Formation from the Yangtze and Cathaysia blocks: Acta Petrological Sinica, v. 29, p. 3592–3606 [in Chinese with an English abstract].

Liew, T.C., and McCulloch, M.T., 1985, Genesis of granitoid batholiths of Peninsular Malaysia and implications for models of crustal evolution: Evidence from Nd-Sr isotopic and U-Pb zircon study: Geochimica et Cosmochimica Acta, v. 49, p. 589–600, https://doi.org/10.1016/0016-7037(85)90050-X.

Liu, H.C., Wang, Y.J., Cawood, P.A., Fan, W.M., Cai, Y.F., and Xing, X.W., 2015, Record of Tethyan Ocean closure and Indosinian collision along the Ailaoshan suture zone (SW China): Gondwana Research, v. 27, p. 1292–1306, https://doi.org/10.1016/j.gr.2013.12.013.

Liu, H.C., Wang, Y.J., and Zi, J.W., 2017, Petrogenesis of the Dalongkai mafic-ultramafic intrusion and its tectonic implication for the Paleotethyan evolution in the Ailaoshan tectonic zone, SW China: Journal of Asian Earth Sciences, v. 141, p. 112–124, https://doi.org/10.1016/j.jseaes.2016.07.015.

Liu, J.L., Tran, M.D., Tang, Y., Nguyen, Q.L., Tran, T.H., Wu, W., Chen, J.F., Zhang, Z.C., and Zhao, Z.D., 2012, Permo-Triassic granitoids in the northern part of the Truong Son belt, NW Vietnam: Geochronology, geochemistry and tectonic implications: Gondwana Research, v. 22, p. 628–644, https://doi.org/10.1016/j.gr.2011.10.011.

Liu, Y.S., Hu, Z.C., Zong, K.Q., Gao, C.G., Gao, S., Xu, J., and Chen, H.H., 2010, Reappraisal and refinement of zircon U-Pb isotope and trace element analyses by LA-ICP-MS: Chinese Science Bulletin, v. 55, p. 1535–1546, https://doi.org/10.1007/s11434-010-3052-4.

Ludwig, K.R., 2003, User's Manual for Isoplot 3.0: Geochronological Toolkit for Microsoft Excel: Berkeley Geochronology Center Special Publication 4, 70 p.

Maluski, H., Lepvrier, C., Leyreloupa, A., Tich, V.V., and Thi, P.T., 2005, ^{40}Ar-^{39}Ar geochronology of the charnockites and granulites of the Kan Nack complex, Kon Tum Massif, Vietnam: Journal of Asian Earth Sciences, v. 25, p. 653–677, https://doi.org/10.1016/j.jseaes.2004.07.004.

Meng, Q.R., and Zhang, G.W., 1999, Timing of collision of the North and South China blocks: Controversy and

reconciliation: Geology, v. 27, p. 123–126, https://doi.org/10.1130/0091-7613(1999)027<0123:TOCOTN>2.3.CO;2.

Metcalfe, I., 1996, Gondwanaland dispersion, Asian accretion and evolution of eastern Tethys: Australian Journal of Earth Sciences, v. 43, p. 605–623, https://doi.org/10.1080/08120099608728282.

Metcalfe, I., 2002, Permian tectonic framework and palaeogeography of SE Asia: Journal of Asian Earth Sciences, v. 20, p. 551–566, https://doi.org/10.1016/S1367-9120(02)00022-6.

Metcalfe, I., 2011, Palaeozoic–Mesozoic history of SE Asia, *in* Hall, R., Cottam, M.A., and Wilson, M.E.J., eds., The SE Asian Gateway: History and Tectonics of the Australia-Asia Collision: Geological Society, London, Special Publication 355, p. 7–35, https://doi.org/10.1144/SP355.2.

Metcalfe, I., 2013, Gondwana dispersion and Asian accretion: Tectonic and palaeogeographic evolution of eastern Tethys: Journal of Asian Earth Sciences, v. 66, p. 1–33, https://doi.org/10.1016/j.jseaes.2012.12.020.

Nie, X.M., Feng, Q.L., Metcalfe, I., Baxter, A.T., and Liu, G.C., 2016, Discovery of a Late Devonian magmatic arc in the southern Lancangjiang zone, western Yunnan: Geochemical and zircon U-Pb geochronological constraints on the evolution of Tethyan ocean basins in SW China: Journal of Asian Earth Sciences, v. 118, p. 32–50, https://doi.org/10.1016/j.jseaes.2015.12.026.

Pang, C.J., Krapež, B., Li, Z.X., Xu, Y.G., Liu, H.Q., and Cao, J., 2014, Stratigraphic evolution of a Late Triassic to Early Jurassic intracontinental basin in southeastern South China: A consequence of flat-slab subduction?: Sedimentary Geology, v. 302, p. 44–63, https://doi.org/10.1016/j.sedgeo.2014.01.003.

Qian, X., Feng, Q.L., Yang, W.Q., Wang, Y.J., Chonglakmani, C., and Monjai, D., 2015, Arc-like volcanic rocks in NW Laos: Geochronological and geochemical constraints and their tectonic implications: Journal of Asian Earth Sciences, v. 98, p. 342–357, https://doi.org/10.1016/j.jseaes.2014.11.035.

Qiu, L., Yan, D.P., Yang, W.X., Wang, J.B., Tang, X.L., and Ariser, S., 2017, Early to Middle Triassic sedimentary records in the Youjiang Basin, South China: Implications for Indosinian orogenesis: Journal of Asian Earth Sciences, v. 141, p. 125–139, https://doi.org/10.1016/j.jseaes.2016.09.020.

Qiu, Y.M., Gao, S., McNaughton, N.J., Groves, D.L., and Ling, W.L., 2000, First evidence of >3.2 Ga continental crust in the Yangtze craton of South China and its implications for Archean crustal evolution and Phanerozoic tectonics: Geology, v. 28, p. 11–14, https://doi.org/10.1130/0091-7613(2000)028<0011:FEOGCC>2.0.CO;2.

Ren, J.S., 1964, A preliminary study on pre-Devonian geotectonic problems of southeastern China: Acta Geologica Sinica, v. 44, p. 418–431.

Ren, J.S., 1991, On the geotectonics of southern China: Acta Geologica Sinica [English edition], v. 4, p. 11–136.

Rubatto, D., 2002, Zircon trace element geochemistry: Partitioning with garnet and the link between U-Pb ages and metamorphism: Chemical Geology, v. 184, no. 1, p. 123–138, https://doi.org/10.1016/S0009-2541(01)00355-2.

Scherer, E., Munker, C., and Mezger, K., 2001, Calibration of the lutetium-hafnium clock: Science, v. 293, p. 683–687, https://doi.org/10.1126/science.1061372.

Segal, I., Halicz, L., and Platzner, I.T., 2003, Accurate isotope ratio measurements of ytterbium by multiple collection inductively coupled plasma mass spectrometry applying erbium and hafnium in an improved double external normalization procedure: Journal of Analytical Atomic Spectrometry, v. 18, no. 10, p. 1217–1223, https://doi.org/10.1039/b307016f.

Shu, L.S., Faure, M., Wang, B., Zhou, X., and Song, B., 2008, Late Palaeozoic–early Mesozoic geological features of South China: Response to the Indosinian collision events in Southeast Asia: Comptes Rendus Geoscience, v. 340, p. 151–165, https://doi.org/10.1016/j.crte.2007.10.010.

Shu, L.S., Zhou, X.M., Deng, P., Wang, B., Jiang, S.Y., Yu, J.H., and Zhao, X.X., 2009, Mesozoic tectonic evolution of the southeast China block: New insights from basin analysis: Journal of Asian Earth Sciences, v. 34, p. 376–391, https://doi.org/10.1016/j.jseaes.2008.06.004.

Shu, L.S., Wang, B., Cawood, P.A., Santosh, M., and Xu, Z.Q., 2015, Early Paleozoic and Early Mesozoic intraplate tectonic and magmatic events in the Cathaysia block, South China: Tectonics, v. 34, p. 1600–1621, https://doi.org/10.1002/2015TC003835.

Sláma, J., Košler, J., Condon, D.J., Crowley, J.L., Gerdes, A., Hanchar, J.M., Horstwood, M.S.A., Morris, G.A., Nasdala, L., Norberg, N., Schaltegger, U., Schoene, B., Tubrett, M.N., and Whitehouse, M.J., 2008, Plešovice zircon—A new natural reference material for U-Pb and Hf isotopic microanalysis: Chemical Geology, v. 249, p. 1–35, https://doi.org/10.1016/j.chemgeo.2007.11.005.

Spencer, C.J., Harris, R.A., and Major, J.R., 2016, Provenance of Permian–Triassic Gondwana sequence units accreted to the Banda arc in the Timor region: Constraints from zircon U-Pb and Hf isotopes: Gondwana Research, v. 38, p. 28–39, https://doi.org/10.1016/j.gr.2015.10.012.

Taylor, B., and Hayes, D.E., 1983, Origin and history of the South China Sea basin, *in* Hayes, D.E., ed., The Tectonic and Geologic Evolution of Southeast Asian Seas and Islands: Part 2: American Geophysical Union Geophysical Monograph 27, p. 23–56. https://doi.org/10.1029/GM027p0023.

Usuki, T., Lan, C.Y., Wang, K.L., and Chi, H.Y., 2013, Linking the Indochina block and Gondwana during the early Paleozoic: Evidence from U-Pb ages and Hf isotopes of detrital zircons: Tectonophysics, v. 586, p. 145–159, https://doi.org/10.1016/j.tecto.2012.11.010.

Veevers, J.J., 2004, Gondwanaland from 650–500 Ma assembly through 320 Ma merger in Pangea to 185–100 Ma breakup: Supercontinental tectonics via stratigraphy and radiometric dating: Earth-Science Reviews, v. 68, p. 1–132, https://doi.org/10.1016/j.earscirev.2004.05.002.

Vervoort, J.D., and Blichert-Toft, J., 1999, Evolution of the depleted mantle: Hf isotope evidence from juvenile rocks through time: Geochimica et Cosmochimica Acta, v. 63, p. 533–556, https://doi.org/10.1016/S0016-7037(98)00274-9.

Vượng, N., Hansen, B.T., Wemmer, K., Lepvrier, C., Tích, V., and Thắng, T.T., 2013, U/Pb and Sm/Nd dating on ophiolitic rocks of the Song Ma suture zone (northern Vietnam): Evidence for Upper Paleozoic Paleotethyan lithospheric remnants: Journal of Geodynamics, v. 69, p. 140–147, https://doi.org/10.1016/j.jog.2012.04.003.

Wan, Y.S., Liu, D.Y., Xu, M., Zhuang, J., Song, B., Shi, Y., and Du, L., 2007, SHRIMP U-Pb zircon geochronology and geochemistry of metavolcanic and metasedimentary rocks in northwestern Fujian, Cathaysia block, China: Tectonic implications and the need to redefine lithostratigraphic units: Gondwana Research, v. 12, p. 166–183, https://doi.org/10.1016/j.gr.2006.10.016.

Wan, Y.S., Liu, D.Y., Wilde, S.A., Cao, J.J., Chen, B., Dong, C.Y., Song, B., and Du, L.L., 2010, Evolution of the Yunkai terrane, South China: Evidence from SHRIMP zircon U-Pb dating, geochemistry and Nd isotope: Journal of Asian Earth Sciences, v. 37, p. 140–153, https://doi.org/10.1016/j.jseaes.2009.08.002.

Wang, G.S., He, F.B., Zhu, W.P., and Ma, W.P., 2009, U-Pb dating of detrital zircons from Late Triassic Wenbinshan Formation in southwestern Fujian and its geological significance: Geoscience, v. 23, p. 246–255 [in Chinese with an English abstract].

Wang, Q.F., Deng, J., Li, C., Li, G.J., Li, Y., and Qiao, L., 2014, The boundary between the Simao and Yangtze blocks and their locations in Gondwana and Rodinia: Constraints from detrital and inherited zircons: Gondwana Research, v. 26, p. 438–448, https://doi.org/10.1016/j.gr.2013.10.002.

Wang, X.F., Metcalfe, I., and Jian, P., 2000, The Jinshajiang-Ailaoshan suture zone, China, tectonostratigraphy, age and evolution: Journal of Asian Earth Sciences, v. 18, p. 675–690, https://doi.org/10.1016/S1367-9120(00)00039-0.

Wang, Y.J., Zhang, Y.H., Fan, W.M., and Peng, T.P., 2005, Structural signatures and $^{40}Ar/^{39}Ar$ geochronology of the Indosinian Xuefengshan tectonic belt, South China block: Journal of Structural Geology, v. 27, p. 985–998, https://doi.org/10.1016/j.jsg.2005.04.004.

Wang, Y.J., Fan, W.M., Sun, M., Liang, X.Q., Zhang, Y.H., and Peng, T.P., 2007a, Geochronological, geochemical and geothermal constraints on petrogenesis of the Indosinian peraluminous granites in the South China block: A case study in the Hunan Province: Lithos, v. 96, p. 475–502, https://doi.org/10.1016/j.lithos.2006.11.010.

Wang, Y.J., Fan, W.M., Cawood, P.A., Ji, S.C., Peng, T.P., and Chen, X.Y., 2007b, Indosinian high-strain deformation for the Yunkaidashan tectonic belt, South China: Kinematics and $^{40}Ar/^{39}Ar$ geochronological constraints: Tectonics, v. 26, TC6008, https://doi.org/10.1029/2007TC002099.

Wang, Y.J., Zhang, F.F., Fan, W.M., Zhang, G., Chen, S.Y., Cawood, P.A., and Zhang, A.M., 2010, Tectonic setting of the SCB in the early Paleozoic: Resolving intracontinental and ocean closure models from detrital zircon U-Pb geochronology: Tectonics, v. 29, TC6020, https://doi.org/10.1029/2010TC002750.

Wang, Y.J., Fan, W.M., Zhang, G.W., and Zhang, Y.H., 2013, Phanerozoic tectonics of the South China block: Key observations and controversies: Gondwana Research, v. 23, p. 1273–1305, https://doi.org/10.1016/j.gr.2012.02.019.

Wang, Y.J., Qian, X., Cawood, P.A., Liu, H.C., Feng, Q.L., Zhao, G.C., Zhang, Y.H., He, H.Y., and Zhang, P.Z., 2018, Closure of the East Paleotethyan Ocean and amalgamation of the Eastern Cimmerian and Southeast Asia continental fragments: Earth-Science Reviews, v. 186, p. 195–230, https://doi.org/10.1016/j.earscirev.2017.09.013.

Weislogel, A.L., Graham, S.A., Chang, E.Z., Wooden, J.L., Gehrels, G.E., and Yang, H.S., 2006, Detrital zircon provenance of the Late Triassic Songpan-Ganzi complex: Sedimentary record of collision of the North and South China blocks: Geology, v. 34, p. 97–100, https://doi.org/10.1130/G21929.1.

Wiedenbeck, M., Alle, P., Corfu, F., Griffin, W.L., Meier, M., Oberli, F., Von, A., Quadt, J., Roddick, C., and Spiegel, W., 1995, Three natural zircon standards for U-Th-Pb, Lu-Hf, trace element and REE analyses: Geostandards Newsletter, v. 19, p. 1–23, https://doi.org/10.1111/j.1751-908X.1995.tb00147.x.

Wu, F.Y., Yang, Y.H., Xie, L.W., Yang, J.H., and Xu, P., 2006, Hf isotopic compositions of the standard zircons and baddeleyites used in U-Pb geochronology: Chemical Geology, v. 234, p. 105–126, https://doi.org/10.1016/j.chemgeo.2006.05.003.

Xia, X.P., Ren, Z.Y., Wei, G.J., Zhang, L., Sun, M., and Wang, Y.J., 2013, In situ rutile U-Pb dating by laser ablation-MC-ICPMS: Geochemical Journal, v. 47, p. 459–468 http://hdl.handle.net/10722/202769, https://doi.org/10.2343/geochemj.2.0267.

Xie, C.F., Zhu, J.C., Ding, S.J., Zhang, Y.M., Fu, T.A., and Li, Z.H., 2006, Identification of Hercynian shoshonitic intrusive rocks in central Hainan Island and its geotectonic implications: Chinese Science Bulletin, v. 51, p. 2507–2519, https://doi.org/10.1007/s11434-006-2122-0.

Xing, X.W., Wang, Y.J., and Zhang, Y.Z., 2016, Detrital zircon U-Pb geochronology and Lu-Hf isotopic compositions of the Wuliangshan metasediment rocks in SW Yunnan (China) and its provenance implication: Journal of Earth Science, v. 27, p. 412–424, https://doi.org/10.1007/s12583-015-0647-3.

Xu, Y.J., Cawood, P.A., Du, Y.S., Huang, H.W., and Wang, X.Y., 2014, Early Paleozoic orogenesis along Gondwana's northern margin constrained by provenance data from South China: Tectonophysics, v. 636, p. 40–51, https://doi.org/10.1016/j.tecto.2014.08.022.

Yan, D.P., Zhou, M.F., Song, H.L., Wang, X.W., and Malpas, J., 2003, Origin and tectonic significance of a Mesozoic multi-layer over-thrust system within the Yangtze bock (South China): Tectonophysics, v. 361, p. 239–254, https://doi.org/10.1016/S0040-1951(02)00646-7.

Yan, Y.G., Huang, B.C., Zhao, J., Zhang, D.H., Liu, X.H., Charusiri, P., and Veeravinantanakul, A., 2017, Large southward motion and clockwise rotation of Indochina throughout the Mesozoic: Paleomagnetic and detrital zircon U-Pb geochronological constraints: Earth and

Planetary Science Letters, v. 459, p. 264–278, https://doi.org/10.1016/j.epsl.2016.11.035.

Yang, J.H., Cawood, P.A., Du, Y.S., Huang, H., and Hu, L.S., 2012, Detrital record of Indosinian mountain building in SW China: Provenance of the Middle Triassic turbidites in the Youjiang Basin: Tectonophysics, v. 574–575, p. 105–117, https://doi.org/10.1016/j.tecto.2012.08.027.

Yang, Z.Y., and He, B., 2012, Geochronology of detrital zircons from the Middle Triassic sedimentary rocks in the Nanpanjiang Basin: Provenance and its geological significance: Geotectonica et Metallogenia, v. 36, p. 581–596 [in Chinese with an English abstract].

Yokoyama, K., Tsutsumi, Y., Nhung, N.T., and Quynh, P.V., 2010, Age distribution of monazites from the nine rivers of Vietnam: Memoirs of the National Museum of Nature and Science, v. 46, p. 97–108.

Yu, J.H., Wang, L.J., Griffin, W.L., O'Reilly, S.Y., Zhang, M., Li, C.Z., and Shu, L.S., 2009, A Paleoproterozoic orogeny recorded in a long-lived cratonic remnant (Wuyishan terrane), eastern Cathaysia block, China: Precambrian Research, v. 174, p. 347–363, https://doi.org/10.1016/j.precamres.2009.08.009.

Yu, J.H., O'Reilly, S.Y., Wang, L.J., Griffin, W.L., Zhou, M.F., Zhang, M., and Shu, L.S., 2010, Components and episodic growth of Precambrian crust in the Cathaysia block, South China: Evidence from U-Pb ages and Hf isotopes of zircons in Neoproterozoic sediments: Precambrian Research, v. 181, p. 97–114, https://doi.org/10.1016/j.precamres.2010.05.016.

Yu, J.H., O'Reilly, S.Y., Zhou, M.F., Griffin, W.L., and Wang, L.J., 2012, U-Pb geochronology and Hf-Nd isotopic geochemistry of the Badu Complex, southeastern China: Implications for the Precambrian crustal evolution and paleogeography of the Cathaysia block: Precambrian Research, v. 222–223, p. 424–449, https://doi.org/10.1016/j.precamres.2011.07.014.

Zaw, K., and Meffre, S., 2007, Metallogenic Relations and Deposit Scale Studies, Final Report: Geochronology, Metallogenesis and Deposit Styles of Loei Fold Belt in Thailand and Laos PDR: Hobart, Australia, ARC Linkage Project, CODES with Industry Partners, University of Tasmania, 302 p.

Zhang, G.W., Guo, A.L., Wang, Y.J., Li, S.Z., Dong, Y.P., Liu, S.F., He, D.F., Cheng, S.Y., Lu, R.K., and Yao, A.P., 2013, Tectonics of South China continent and its implications: Science China, v. 56, no. 11, p. 1804–1828, https://doi.org/10.1007/s11430-013-4679-1.

Zhang, L., Ren, Z.Y., Alexander Nichols, A.R.L., Zhang, Y.H., Zhang, Y., Qian, S.P., and Liu, J.Q., 2014, Lead isotope analysis of melt inclusions by LA-MCICP-MS: Journal of Analytical Atomic Spectrometry, v. 29, p. 1393–1405, https://doi.org/10.1039/C4JA00088A.

Zhang, L.M., Wang, Y.J., Zhang, Y.Z., Liu, H.C., and Zhang, X.C., 2017, Age of Paleozoic strata in northern Hainan Island: Constraints from the detrital zircon U-Pb geochronology: Journal of Jilin University (Earth Science Edition), v. 47, p. 1187–1206, https://doi.org/10.13278/j.cnki.jjuese.201704116 [in Chinese with an English abstract].

Zhang, X.C., Huang, C.Y., Wang, Y.J., Clift, P.D., Yan, Y., Fu, X.W., and Chen, D.F., 2017, Evolving Yangtze River reconstructed by detrital zircon U-Pb dating and petrographic analysis of Miocene marginal sea sedimentary rocks of the Western Foothills and Hengchun Peninsula, Taiwan: Tectonics, v. 36, no. 4, p. 634–651, https://doi.org/10.1002/2016TC004357.

Zhang, X.C., Wang, Y.J., Clift, P.D., Yan, Y., Zhang, Y.Z., and Zhang, L., 2018, Paleozoic tectonic setting and paleogeographic evolution of the Qin-Fang region, southern South China block: Detrital zircon U-Pb geochronological and Hf isotopic constraints: Geochemistry Geophysics Geosystems, v. 19, p. 3962–3979, https://doi.org/10.1029/2018GC007713.

Zhao, G.C., and Cawood, P.A., 1999, Tectonothermal evolution of the Mayuan assemblage in the Cathaysia block: New evidence for Neoproterozoic collision-related assembly of the South China craton: American Journal of Science, v. 299, p. 309–339, https://doi.org/10.2475/ajs.299.4.309.

Zheng, H.B., Clift, P.D., Wang, P., Tada, R., Jia, J., He, M., and Jourdan, F., 2013, Pre-Miocene birth of the Yangtze River: Proceedings of the National Academy of Sciences of the United States of America, v. 110, no. 19, p. 7556–7561, https://doi.org/10.1073/pnas.1216241110.

Zheng, J.P., Griffin, W.L., O'Reilly, S.Y., Zhang, M., Pearson, N., and Pan, Y.M., 2006, Widespread Archean basement beneath the Yangtze craton: Geology, v. 34, p. 417–420, https://doi.org/10.1130/G22282.1.

Zhou, X.M., and Li, W.X., 2000, Origin of late Mesozoic igneous rocks in southeastern China: Implications for lithosphere subduction and underplating of mafic magmas: Tectonophysics, v. 326, p. 269–287, https://doi.org/10.1016/S0040-1951(00)00120-7.

Zhu, K.J., Li, Z.X., Xu, X.S., and Wilde, S.A., 2014, A Mesozoic Andean-type orogenic cycle in southeastern China as recorded by granitoid evolution: American Journal of Science, v. 314, no. 1, p. 187–234, https://doi.org/10.2475/01.2014.06.

Zi, J.W., Cawood, P.A., Fan, W.M., Wang, Y.J., and Tohver, E., 2012, Contrasting rift and subduction-related plagiogranites in the Jinshajiang ophiolitic mélange, southwest China, and implications for the Paleo-Tethys: Tectonics, v. 31, TC2012, https://doi.org/10.1029/2011TC002937.

Science Editor: Rob Strachan
Associate Editor: Anna Bird

Manuscript Received 8 May 2018
Revised Manuscript Received 17 October 2018
Manuscript Accepted 7 December 2018

Printed in the USA